DOCTORAL THESIS

Geochemistry and Mineralogy of Acid Sulfate Soils in northern Sweden: Elemental distribution and groundwater chemistry

Federico Alvarellos

Applied Geochemistry

LULEÅ UNIVERSITY OF TECHNOLOGY

Geochemistry and Mineralogy of Acid Sulfate Soils in northern Sweden: Elemental distribution and groundwater chemistry

Federico Alvarellos

Division of Geosciences and Environmental Engineering, Applied Geochemistry

Department of Civil, Environmental, and Natural Resources Engineering
Luleå University of Technology
Luleå, Sweden

December 2025

Supervisors: Lena Alakangas and Sarah Conrad

Cover picture:

Photograph from the water sampling campaign in Södra Sunderbyn (2023). The reddish-coloration of the water is indicative of oxidation processes occurring in the surrounding sulfide-bearing sediments. Photograph by Federico Alvarellos.

Acid sulfate soils (AS-soils) refer to soils or fine-grained sulfide-bearing sediments that can produce acidity through sulfide oxidation. AS-soils do not pose a risk under waterlogged conditions, but when exposed to oxygen, negative environmental and economic impacts are generated. AS-soils oxidation results in sulfuric acid production, water bodies acidification, elements mobilization within the soil and into water bodies, adverse effects on biota, infrastructure damages, and potential deleterious effects on human health. Studying AS-soils presents a significant challenge due to their widespread impacts, highlighting the need for efforts to mitigate their environmental consequences. This doctoral thesis investigated the geochemical and mineralogical characteristics of AS-soils in northern Sweden, aiming to enhance understanding of their characteristics and weathering processes and thus contribute to developing environmental management strategies.

AS-soils represent a global concern due to their extensive distribution, mainly in coastal areas that were once covered by saline or brackish water. In Sweden, AS-soils are distributed along the coastline and are derived from post-glacial sediments enriched with Fe sulfides. In the Baltic Sea, sulfide-bearing sediments are exposed to oxygen due to post-glacial isostatic uplift or groundwater table lowering. In Sweden, AS-soils are already oxidized, posing environmental risks that are further intensified in northern regions due to a greater rate of isostatic uplift. AS-soils are characterized by the accumulation of elements in a transition zone (TZ) between oxidized and reduced sediments. The oxidized zone (OZ) is distinguished by low pH values (< 4), element depletion, and the precipitation of Fe (oxy)hydroxide and Fe hydroxysulfate secondary minerals as common products of sulfide oxidation. In contrast, the reduced zone (RZ) represents the AS-soil parent material and consists of unoxidized black, fine-grained laminated sediments, characterized by a high total organic carbon content, high S content, and abundance of primary Fe sulfide minerals. Groundwater fluctuations influence soil redox conditions and pH, causing the transformation of unoxidized sediments into oxidized ones. This zone transformation induces the dissolution and reprecipitation of minerals, leading to element mobilization.

This study analyzed AS-soils in Luleå, northern Sweden, from a geochemical and mineralogical perspective. Research on soil and groundwater was conducted in one waterlogged (SW) and one oxidized (SN) AS-soil profile located in Södra Sunderbyn, in the vicinity of the Lule River. Elemental distribution over the different zones was analyzed, identifying depletion and accumulation zones, and assessing the mobilized elements as potential contaminants in soil and water bodies. Mineralogical analyses were conducted through techniques such as scanning electron microscopy (SEM), X-ray diffraction (XRD), and microprobe, which were applied with the aim of identifying primary and secondary minerals, their composition, textures, morphologies, and distribution over the zones, and their impact on soil chemistry under weathering conditions. Furthermore, sequential extraction experiments were performed to associate the elements with each of the soil fractions and to quantify the potential elements released under oxidation. Additionally, interactions between groundwater and subsoil were evaluated, identifying sources and element mobilization pathways, acting as potential contaminants.

The results demonstrated that both AS-soil profiles have the potential to generate acidity and mobilize elements upon exposure to oxygen, posing a negative environmental impact. Different S species were identified across the soil profiles. In unoxidized samples, S mainly occurs as primary Fe sulfide, metastable Fe sulfide, and organic S. Framboidal pyrite, the most abundant sulfide mineral and the primary acidity contributor, precipitated under anoxic-euxinic conditions through microbial sulfate reduction (MSR), as evidenced by negative $\delta^{34}S$ values. In contrast, oxidized samples predominantly contain S in secondary Fe hydroxysulfate minerals, such as jarosite or schwertmannite, which display negative $\delta^{34}S$ values indicative of sulfide oxidation processes, associated with their precursor sulfide.

Incubation experiments over the profiles showed that pH decreases the most in samples with high S content, but not necessarily with high TOC content. In this research, it is demonstrated that framboidal pyrite is highly reactive and prone to rapid oxidation even with short periods of exposure to oxygen. Compositional maps obtained by microprobe analysis indicated that framboidal pyrite is a source of Cu, Mn, Mo, and Ni. These trace elements are typically distributed within the framboids, except for Mn, which surrounds the framboids, creating a Mn-rich rim. The labile and more stable organic fraction is strongly associated with Cu, Mo, and S, which are susceptible to mobilization during weathering. Despite past oxidation and element mobilization occurring in the OZ, this zone still exhibited a high percentage of elements with potential to be removed as shown in the extraction experiments. The most soluble phases and pore water contribute with high concentrations of Cd, Cu, Mn, Mo, and S, indicating their high potential for environmental release.

Seasonal variations result in groundwater fluctuations exposing the sulfide-bearing sediments to oxygen as the water table decreases, leading to oxidation and acidification. In contrast, during high water table periods, secondary mineral dissolution and element mobilization take place. These fluctuated redox conditions were evidenced by variations in $\delta^{56}Fe$ groundwater values, due to dissolution and transformation of Fe phases. The SN well registered high concentrations of Al, Co, Fe, Mn, Ni, S, and Zn in May and October, during low groundwater table periods. In contrast, the SW well remained waterlogged, preventing oxidation and acidity generation. The difference between the wells is evidenced by $\delta^{34}S$ values, with the SW well showing strong ^{34}S enrichment from active MSR, while the SN well reflects dominant sulfide oxidation and limited MSR activity.

This study shows the environmental risks associated with sulfide oxidation in northern Sweden and demonstrates that maintaining sulfide-bearing sediments under waterlogged conditions is essential to limit oxygen exposure, reduce acid generation, maintain alkaline pH levels, and minimize the release of dissolved elements, thereby mitigating negative environmental impacts.

Keywords: framboidal pyrite, acidity, element mobilization, groundwater, organic matter.

Completing this doctoral program has been a profound process of both professional and personal growth. Over the course of these years, laboratory work, field campaigns, travels, conference presentations, participation in specialized courses, and the preparation of scientific publications have all been fundamental experiences that contributed to my development as a professional.

I would like to express my sincere gratitude to the Division of Applied Geochemistry at Luleå University of Technology (LTU) for the time shared, the ongoing collaboration, and the stimulating and supportive work environment. I am also grateful to the entire university community for their support and for being part of this journey.

My deepest appreciation is extended to my supervisors, Professor Lena Alakangas and Dr. Sarah Conrad, for giving me the opportunity to pursue this PhD and to take part in the acid sulfate soils project in Sweden. Their trust, guidance, expertise, and continuous support were essential to achieving the project's goals. I would also like to acknowledge Professor Björn Öhlander and Dr. Katerina Rodiouchkina for their dedication to the project's development, their valuable input to the scientific publications, and the knowledge they generously shared.

I am profoundly grateful to my family, friends, and my partner, María Fernanda Salto, for their unconditional support and encouragement throughout this entire process.

Finally, I would like to thank all the individuals, institutions, and media outlets that contributed to the dissemination of my research through interviews, publications, and various science outreach initiatives. Their efforts have been key to bringing the knowledge generated closer to a broader audience.

To all of you, thank you.

The thesis is based on the following papers:

I - Alvarellos, F., Conrad, S., Öhlander, B., Alakangas, L., 2024. Geochemical and mineralogical characterization of acid sulfate soils in Luleå, northern Sweden. Journal of Geochemical Exploration. Volume 265, 107541. https://doi.org/10.1016/j.gexplo.2024.107541.

II - Alvarellos, F., Rodiouchkina, K., Conrad, S., Öhlander, B., Alakangas, L., 2025.a. Sources of Element Release from Acid Sulfate Soils to the Environment: Elemental and Mineralogical Evidence from Northern Sweden. https://doi.org/10.1016/j.apgeochem.2025.106571.

III - Alvarellos, F., Conrad, S., Öhlander, B., Alakangas, L., 2025.b. Seasonal variability in groundwater hydrogeochemistry in acid sulfate soils, northern Sweden. (Manuscript)

IV - Conrad, S., Rodiouchkina, K., Alvarellos, F., Öhlander, B., Alakangas, L., 2025. Isotopic insights into iron and sulfur cycling in acid sulfate soils: Implications of seasonal redox fluctuations. (Under review)

Peer-reviewed conference abstracts:

These conference abstracts are not included in the thesis.

I - Alvarellos, F., Conrad, S., Alakangas, L., (2022). Differences in the mineralogy and geochemical composition of oxidized and waterlogged acid sulphate soils in northern Sweden. Conference paper presented at Glasgow World Soil Science Congress. Glasgow, Scotland.

II - Alvarellos, F., Conrad, S., Alakangas, L., (2022). Differences in the mineralogy and geochemical composition of oxidized and waterlogged acid sulphate soils in northern Sweden. Conference paper presented at Swedish Geological Congress. Uppsala, Sweden.

III - Alvarellos, F., Conrad, S., Alakangas, L., (2023). Geochemical and mineralogical composition of acid sulfate soils in Luleå, northern Sweden. Conference paper presented at the 9th International Acid Sulfate Soils Conference. Adelaide, Australia.

AAS-Soils: Active acid sulfate soils

AS-soils: Acid sulfate soils

DOC: Dissolved organic carbon

EC: Electrical conductivity

FEG-EPMA: Field Emission Gun Electron Probe Microanalyzer

ICP-SFMS: Sector Field Inductively Coupled Plasma Mass Spectrometry

LDO: Luminescent dissolved oxygen

MC-ICP-MS: Multi-Collector Inductively Coupled Plasma Mass Spectrometry

OZ: Oxidized zone

PAS-Soils: Potential acid sulfate soil

pHf: Field pH

pHi: Incubation pH

RZ: Reduced zone

SEM-EDS: Scanning Electron Microscope-Energy Dispersive Spectroscopy

SN: Oxidized profile

SW: Waterlogged profile

TZ: Transition zone

XRD: X-Ray Diffraction

Part I

Part II

Paper I - Geochemical and mineralogical characterization of acid sulfate soils in Luleå, northern Sweden. 2024. Authors: Alvarellos, F., Conrad, S., Öhlander, B., Alakangas, L.

Paper II - Sources of Element Release from Acid Sulfate Soils to the Environment: Elemental and Mineralogical Evidence from Northern Sweden. 2025.a. Authors: Alvarellos, F., Rodiouchkina, K., Conrad, S., Öhlander, B., Alakangas, L.

Paper III - Seasonal variability in groundwater hydrogeochemistry in acid sulfate soils, northern Sweden. 2025.b. Authors: Alvarellos, F., Conrad, S., Öhlander, B., Alakangas, L.

Paper IV - Isotopic insights into iron and sulfur cycling in acid sulfate soils: Implications of seasonal redox fluctuations. 2025. Authors: Conrad, S., Rodiouchkina, K., Alvarellos, F., Öhlander, B., Alakangas, L.

Contribution to the Appended Papers:

Paper I - Investigation and Methodology: Installation of sampling stations, collection of acid sulfate soil profiles, and sample processing were performed by Federico Alvarellos, Sarah Conrad, and members of the Applied Geochemistry Division. **Formal analysis:** Mineralogical analyses were conducted by Federico Alvarellos with support from the Applied Geochemistry Division. **Conceptualization, Writing, Review and Editing – original draft:** Federico Alvarellos, Sarah Conrad, Björn Öhlander, and Lena Alakangas contributed to the conceptual framework, data interpretation, manuscript preparation, revision and final editing of the paper.

Paper II - Investigation and Methodology: The sequential extraction experiment was designed and executed by Katerina Rodiouchkina and Federico Alvarellos. **Formal analysis:** Mineralogical analyses were performed by Federico Alvarellos together with members of the Applied Geochemistry Division. **Conceptualization, Writing, Review and Editing – original draft:** Federico Alvarellos, Katerina Rodiouchkina, Sarah Conrad, Björn Öhlander, and Lena Alakangas contributed to the conceptual framework, data interpretation, manuscript preparation, revision and final editing of the paper.

Paper III - Investigation and Methodology: Fieldwork, including groundwater sampling and measurement of physical parameters, was performed by Federico Alvarellos, Sarah Conrad, and members of the Applied Geochemistry Division. **Conceptualization, Writing, Review and Editing – original draft:** Federico Alvarellos, Sarah Conrad, Björn Öhlander, and Lena Alakangas contributed to the conceptual framework, data interpretation, manuscript preparation, revision and final editing of the paper.

Paper IV - Investigation and Formal analysis: Isotopic analyses of sequential extraction samples were conducted by Katerina Rodiouchkina. **Conceptualization, Writing, Review and Editing – original draft:** Sarah Conrad, Katerina Rodiouchkina, Federico Alvarellos, Björn Öhlander, and Lena Alakangas contributed to the conceptual framework, data interpretation, manuscript preparation, revision and final editing of the paper.

1.1 Acid sulfate soils: Definition and Formation

Acid sulfate soils (AS-soils) are fine-grained sediments enriched with Fe sulfides, which can generate acidity through sulfide oxidation (Öborn, 1989). Under waterlogged conditions, these reduced sediments remain stable and are referred to as potential acid sulfate soils (PAS-soils). However, when exposed to oxygen, the sulfides oxidize, producing acid and transforming the sediments into active acid sulfate soils (AAS-soils) (Dent and Pons, 1995). AS-soils profiles exhibit different zones according to their different oxidation degrees: a reduced zone (RZ), a transition zone (TZ), and an oxidized zone (OZ) (Fig. 1a).

AS-soils are found worldwide, particularly in coastal regions, anoxic wetlands, tidal swamps, and lake sediments (Van Breemen, 1980; Dent and Pons, 1995; Andriesse and van Mensvoort, 2002; Becher et al., 2019). In Europe, they are mostly concentrated around the Baltic Sea. For instance, AS-soils cover approximately 2,000 km² in the northern Swedish counties of Norrbotten and Västerbotten (Swedish Geological Survey, SGU). Moreover, AS-soils were also confirmed in regions of southern Sweden (Nyman et al., 2023). Around 1,400 km² is agricultural land affected by AS-soils (Öborn, 1994).

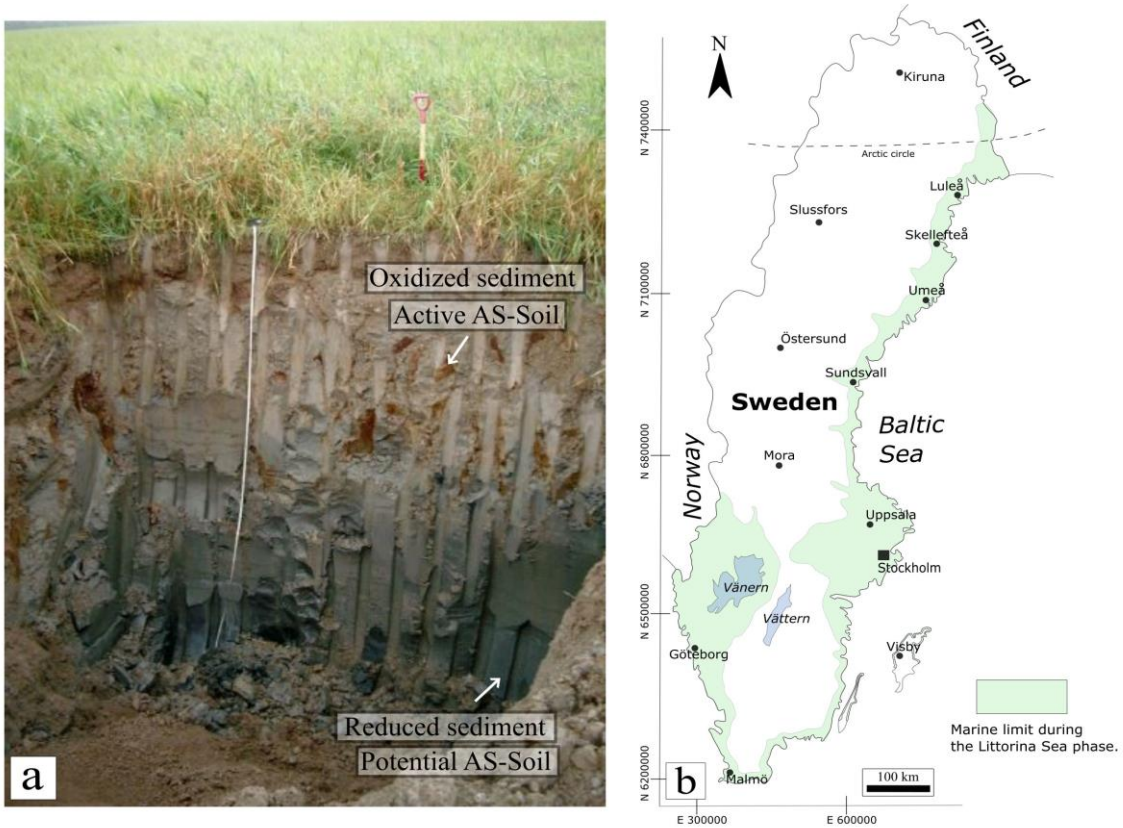

Fig. 1. (a) Modified image of an AS-soil profile in Västerbotten (SGU). The soil profile differentiates the unoxidized, reduced sediments that form the potential AS-soil from the oxidized sediments that constitute the Active AS-soil. (b) Map of Sweden illustrating the extent of the Littorina Sea phase during the Quaternary. The distribution represents the potential areas in which AS-soil can be found. Reference system: SWEREF 99 TM© Swedish Land Survey and SGU. Modified from Lindström, 2017.

AS-soils along the Swedish coastline originated from post-glacial sediments enriched in Fe sulfides during the Littorina Sea phase (7500–4000 BP), a brackish phase in the history of the Baltic Sea (Sohlenius, 1996). These parent sediments developed under anoxic to euxinic conditions, characterized by high concentrations of TOC, Mo, and S (Alvarellos et al., 2024). In such oxygen-depleted marine environments rich in organic material, biogeochemical processes drive the reduction of SO_4^{2-} and Fe^{3+}, leading to the formation of Fe sulfides.

Sulfate-reducing bacteria play a key role in this process by using organic matter as an electron donor to reduce SO_4^{2-} to H_2S (Berner, 1983; Berner, 1985). During this microbial reaction, the organisms derive energy by oxidizing organic matter to CO_2, while simultaneously reducing SO_4^{2-} to H_2S, as shown in Equation 1.

$$SO_4{}^{2-}{}_{(aq)} + 2CH_2O_{(s)} \rightarrow 2HCO^-{}_{3\,(g)} + H_2S_{(g)} \quad (1)$$

The H_2S can migrate upward, downward, or laterally or react with dissolved Fe^{2+} to form Fe sulfides (Berner, 1985). The amount of pyrite that will be precipitated is limited by the supply of organic matter decomposition, dissolved SO_4^{2-}, and dissolved Fe (Berner, 1983).

Under anaerobic environments, microbial reduction of Fe(oxy)hydroxides occurs while organic matter decomposes (Lovely and Phillips, 1986) (Eq. 2).

$$FeOOH_{(s)} + 3CH_2O_{(s)} \rightarrow Fe^{2+}{}_{(aq)} + 3CO_{2\,(g)} + 2H_2O_{(l)} \quad (2)$$

Once Fe^{2+} and H_2S have formed, they can react with each other to form Fe sulfides (Berner, 1983; Berner, 1985) (Eq. 3 and 4).

$$Fe^{2+}{}_{(aq)} + H_2S_{(g)} \rightarrow FeS_{(s)} + 2H^+ \quad (3)$$

$$FeS_{(s)} + H_2S_{(g)} \rightarrow FeS_{2\,(s)} + 2H^+ \quad (4)$$

1.2 Sulfide oxidation and environmental impact

AS-soils can become exposed to oxygen through both natural processes and anthropogenic activities. Natural factors include extreme drought conditions (Fanning et al., 2017) and post-glacial isostatic uplift, which can raise land at rates of 9–10 mm per year in regions such as the northern Bothnian Bay (Johansson et al., 2004; Kaniuth and Vetter, 2004). Human-induced changes, including agricultural drainage (Öborn, 1989), deforestation, and infrastructure development, can also lower groundwater table levels, thereby generating sulfide minerals oxidation (Dent and Pons, 1995). In northern Sweden, a combination of isostatic uplift and anthropogenic lowering of the groundwater table, primarily through cultivation and construction, has led to the exposure of formerly submerged sediments above sea level (Österholm and Åström, 2004; Boman et al., 2010).

The zone at which oxidation processes begin, termed the oxidation front, is situated between the OZ and TZ (Fig. 2). The TZ in the AS-soil profile contains partially saturated sediments that are sensitive to fluctuations in groundwater levels. These fluctuations impact soil redox conditions and pH, facilitating the transformation of unoxidized sediments into oxidized ones. This process leads to mineral dissolution, mobilization of elements and subsequent reprecipitation, and depletion of certain elements (Alvarellos et al., 2024). Elements such as Cd, Co, Ni, S, and Zn become more mobile under acidic conditions, and can leach into water bodies or redistribute within the soil profile, especially as pH levels increase in the TZ, as shown in

Alvarellos et al (2024). Previous studies have reported the accumulation of elements such as Co, Fe, Mn, Ni, S, and Zn in the TZ (Sohlenius et al., 2015; Sohlenius and Öborn, 2004). Additional research has also documented the mobilization and subsequent accumulation of Co, Ni, and Zn within sulfide-bearing sediments in Finnish coastal areas, particularly in the TZ (Åström, 1998).

Seasonal groundwater variations, driven mainly by rainfall and snowmelt, affect water and soil chemistry by dissolving and precipitating minerals (Johnston et al., 2003; Vithana et al., 2015). During periods of groundwater table decline, sulfide-bearing sediments are exposed to oxygen, leading to oxidation and acidification. In contrast, a rising groundwater table can lead to secondary minerals dissolution, facilitating the elements' mobilization.

The pyrite oxidation by oxygen and water generates sulfuric acid and Fe(III)precipitates, as shown by the following reaction (Nordstrom, 2011) (Eq. 5):

$$FeS_2 + \frac{15}{4}\, O_2 + \frac{7}{2} H_2O \rightarrow Fe(OH)_{3(s)} + 2H_2SO_4 \qquad (5)$$

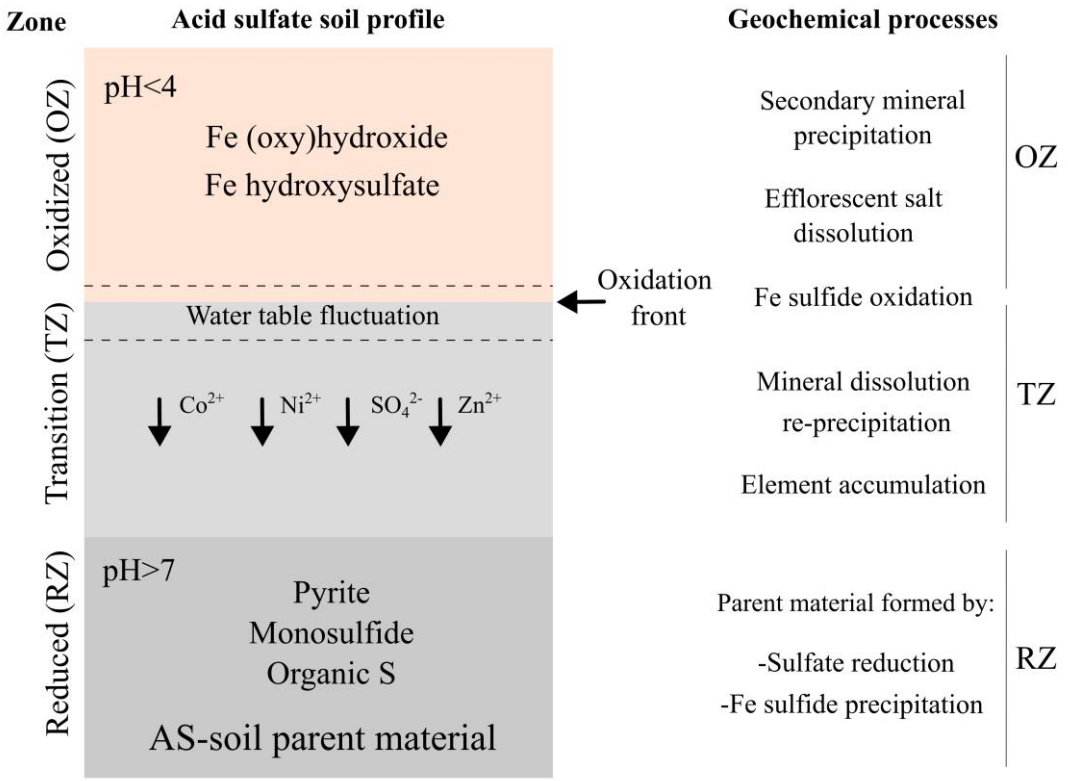

Fig. 2. Illustration of an AS-soil profile with the geochemical processes occurring in each of the distinct zones, driving the sulfide oxidation, elements mobilization, and accumulation, as well as the dissolution and precipitation of mineral phases.

The oxidation of sulfide-bearing sediments generates a significant negative impact on the surrounding environment. Common consequences include compositional changes in soil and water, acidification of adjacent soils and water bodies, corrosion of infrastructure (White et al., 1996), element mobilization into the environment (Åström, 1998; Åström, 2001a; Åström, 2001b; Gröger et al., 2011), and deleterious effects on human health (E.g., multiple sclerosis, Åström and Roos, 2022). The resulting release of metals and dissolved SO_4^{2-} poses ecological risks by harming vegetation and aquatic life, while also contaminating both groundwater and surface water systems (Dent and Pons, 1995).

AS-soils also have ecological implications, particularly in the Baltic Sea, where they have been observed notably concerning fish growth (Hudd and Kjellman, 2002). In terrestrial and aquatic environments near AS-soil areas, elevated metal concentrations have been detected in crops and aquatic plants, with Al, Co, Mn, and Ni among the most frequently observed elements (Fältmarsch et al., 2008; Öhlander et al., 2014). Additionally, studies from southern Sweden have documented high concentrations of metals, including Al, Co, and rare earth elements (REE) in both water and sediment samples affected by AS-soils (Shahabi-Ghahfarokhi et al., 2022).

Climate plays a critical role in the development of AAS-soils, particularly in high-latitude regions such as the Arctic and Antarctica, where sulfidic sediments are often covered by permafrost. The presence of permafrost greatly reduces leaching (Gjorup et al., 2020). In Antarctica, where a semiarid polar climate governs seasonal thawing, monitoring of the active layer reveals that sulfurization and oxidation processes are tightly coupled with climatic variability and permafrost dynamics (Michel et al., 2012). Similarly, in the Russian Arctic, recent findings demonstrate that climate-driven permafrost thaw significantly enhances sulfide oxidation (Kemeny et al., 2023). Thawing processes expose previously frozen, sulfide-bearing sediments to oxygen, triggering oxidation. In both polar regions, permafrost acts as a critical environmental barrier. Its degradation under changing climatic conditions is accelerating the formation of AAS-soils, with negative environmental impacts.

1.3 Isotopes

Geochemical processes including sulfide oxidation, element mobility, and redox-driven transformations in AS-soils can be distinguish through stable isotopic analysis, particularly using $\delta^{56}Fe$ and $\delta^{34}S$ signatures. The combined use of Fe and S isotopic compositions serves as a geochemical tracer for enhancing the understanding of biogeochemical processes. While both isotopic systems may indicate processes such as pyrite oxidation and secondary mineral precipitation, S isotopes are particularly effective in tracing parent materials, whereas Fe isotopes more directly capture redox dynamics (Seal et al., 2000; Bottrell et al., 2008; Ódri et al., 2020).

Isotopes are atoms of the same element with identical atomic numbers but different masses due to varying numbers of neutrons. The delta (δ) notation is used to quantify the relative difference in isotope proportions, as shown in equation 6. Certified reference materials are used in the δ notation; for instance, $\delta^{34}S$ values are reported relative to the IAEA-S1 (International Atomic Energy Agency, Austria) or the V-CDT (Vienna Canyon Diablo Troilite) scale, while $\delta^{56}Fe$ values are referenced against the IRMM-014 (Institute of Reference Materials and Measurements, Belgium). These δ values, expressed in per mil (‰), represent deviations in isotope ratios relative to these standards and can provide insights into geochemical processes.

Equation 6

$$\delta\,{}^{X}R \quad = \left(\frac{R_{sample}}{R_{STD}} - 1\right) * 1000 \qquad (6)$$

R_{sample}: Isotopic ratio in the sample (Heavy isotope / light isotope).

R_{STD}: Isotopic ratio in the international standard.

1.4 Research aim and scope

Given the significant environmental impacts associated with the oxidation of AS-soils and the limited research on mineralogy, element behavior in solid and aqueous phases, and the role of organic matter in the study area, this research aims to enhance the understanding of AS-soils in Luleå, northern Sweden. By integrating geochemical and mineralogical analyses, the study will provide a comprehensive perspective on the processes occurring in AS-soils, offering valuable insights for the development of models and management strategies for these soils.

The specific objectives of this research were:

- Mineralogical and geochemical characterization of AS-soils in northern Sweden (Paper I).
- Provide an understanding of geochemical processes in AS-soils between primary and secondary minerals and soil chemistry (Papers I, II & IV).
- Identify the source and mobilization of elements that can be potential contaminants in soil and water bodies (Papers II & III).
- Evaluate the interaction between the groundwater and the subsoil related to natural or artificial processes (Papers III & IV).

2. Methodology

2.1 Study area

The research on AS-soils was conducted in Södra Sunderbyn, situated 10 km north of Luleå along Sweden´s coastline (Fig. 3). The region is characterized by a flat topography, with an average elevation of 5 meters above sea level. Coniferous forests dominate the landscape, alongside areas of agriculture, housing, and industry. The Lule River, which flows 460 km from the Scandinavian Caledonian Mountains in northwest Sweden to the Gulf of Bothnia in the southeast, is the primary water body in the area. The river's drainage basin covers 24,900 km². Annual precipitation ranges from 400 to 700 mm, with a low evapotranspiration rate (Raab and Vedin, 1995). Approximately 45 % of the precipitation falls as snow, which accumulates during the winter months and typically melts in May (Drugge et al., 2003).

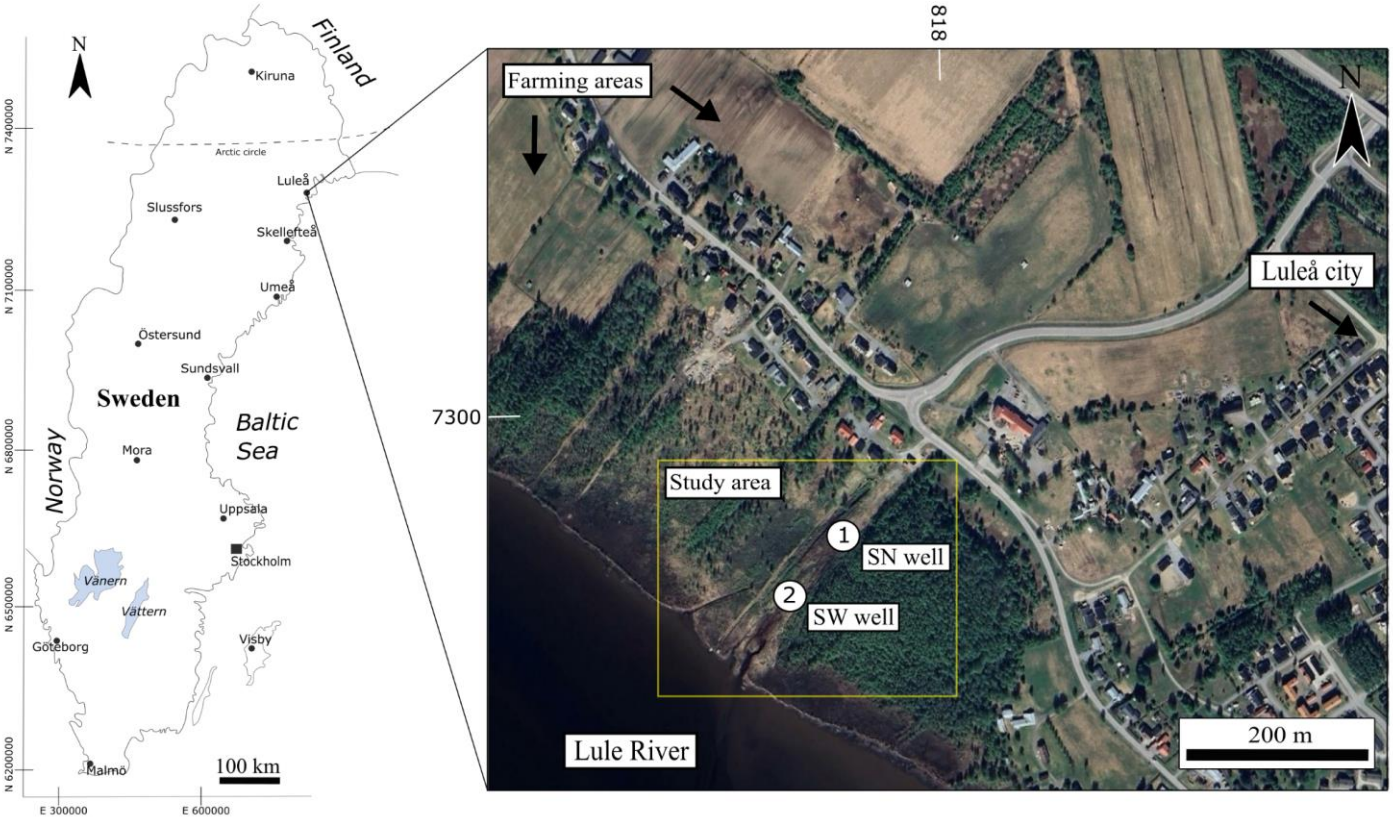

Fig. 3. Satellite image of the study area and the distribution of the two analyzed wells (SN and SW). SWEREF 99 TM Coordinates. Site 1: N 7299828; E 817950. Site 2: N 7299729; E 817897. Google Earth image. (Alvarellos et al., 2025a).

The geology of the region is dominated by Precambrian crystalline and metamorphic rocks, aged between 1.8 and 2.7 billion years, which are overlain by till and postglacial sediments (sgu.se). Quaternary deposits are primarily composed of silty and clay-rich soils, which are associated with the presence of AS-soils. In northern Sweden, these fine-grained materials are frequently covered by fluvial or wave-washed sediments (Sohlenius et al., 2004).

At the sampling site, the soils are mainly composed of clay and silt, forming arable land (Fromm, 1965). AS-soils in northern Sweden have been identified in both agricultural and forested areas (Sohlenius et al., 2015). Postglacial sulfidic sediments, commonly found in clay and silt-rich areas, are often covered by young fluvial deposits or peat layers, which prevent oxidation (Sohlenius et al., 2015). The AS-soil profiles examined in this study consist of fine-grained (Clay and/or silt) sediments with varying oxidation degrees, underlain by sandy deposits.

2.2 Sampling and sample preparation

Two soil profiles were selected for soil and groundwater sampling: one oxidized (SN) and one waterlogged (SW), separated by 100 m (Fig. 4).

2.2.1 Soil sampling

Soil sampling was conducted in June 2022 using a trailer-mounted hydraulic drill to extract two core samples, each with a diameter of 50 mm and a length of 1.2 m. At each site, two boreholes were drilled, one specifically for immediate measurements to minimize the effects of rapid Fe sulfide oxidation. The SW and SN profiles extended to depths of 5.3 m and 6.0 m, respectively. To ensure representative sampling and obtain sufficient material for laboratory analyses, each core was divided into 15 cm sub-samples. Physical and chemical parameters were analyzed, including pH, total element concentration, total organic carbon (TOC), and Fe and S isotopic compositions. In addition, four sub-samples from distinct zones (OZ, TZ, RZ) were selected for detailed mineralogical and chemical characterization. Epoxy sections were prepared following detailed procedures outlined in Alvarellos et al. (2024).

2.2.2 Groundwater sampling

Biweekly groundwater sampling was conducted during the ice-free season, from May 2023 to June 2024, at monitoring wells SN and SW. Samples were collected using a peristaltic pump and filtered through 0.2 µm Whatman cellulose nitrate membranes. Detailed procedures for equipment preparation and groundwater sampling are provided in the manuscript by Alvarellos et al. (2025b). Field parameters recorded included pH, EC, LDO, and temperature. Additional laboratory analyses were performed to determine total element concentration, dissolved organic carbon (DOC), element speciation, and Fe and S isotopic compositions.

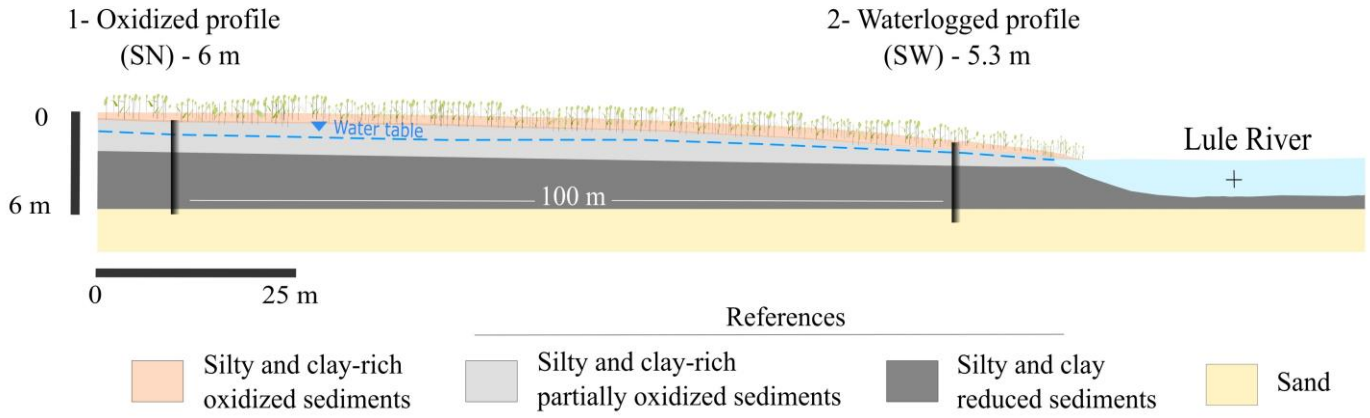

Fig. 4. Schematic diagram of the spatial distribution of the two soil profiles and the different zones according to their oxidation degree (Modified from Alvarellos et al., 2024).

2.3 Geochemical and mineralogical analysis

Table 1. Summary of the different methods, analyzed parameters, and their analytical purposes in AS-soils, as applied in different scientific papers.

Method /Parameter	Objective	Reference paper
pHf and pHi were measured in solid samples. pH, EC, LDO, and T° were recorded during each groundwater sampling event.	To differentiate and classify the AS-soil zones and materials. To determine pH, EC, LDO, and T° in groundwater wells.	I, III
Quantitative element screening of solid and water phases using a sector field inductively coupled plasma mass spectrometry (ICP-SFMS).	To determine the total elemental content in soils and its concentrations in water samples. To calculate the speciation of HCO_3^-, Cl^-, F^-, SO_4^{2-}, S^{2-}, PO_4^{3-}, NH_4^+, and NO_3^- in groundwater.	I, II, III
Quantitative carbon analysis in solid and water phases using IR detection.	To quantify TOC in solid samples and DOC in groundwater.	I, II, III
Scanning electron microscopy – energy dispersive spectroscopy (SEM–EDS)	To identify mineral phases, textures, zonation, and chemical composition in OZ, TZ, and RZ samples.	I, II
X-Ray diffraction (XRD)	To identify and quantify mineral phases, particularly silicates, in OZ, TZ, and RZ samples.	I, II
Field emission gun electron probe microanalyzer (FEG-EPMA)	To perform quantitative microanalysis of As, Cd, Co, Cr, Cu, Fe, Mn, Mo, Ni, Pb, S, and Zn, and to map pyrite composition.	II
Sequential extraction procedure	To evaluate element release and its association with specific soil fractions.	II
Quantitative element screening from pore water using ICP-SFMS.	To assess the bioavailability of elements in pore water under oxidizing conditions.	II
Quantification of Fe and S isotopes in solid and water phases using a multi-collector inductively coupled plasma mass spectrometry (MC-ICP-MS)	To differentiate geochemical processes occurring in solid and aqueous phases	IV

3.1. Geochemical characterization of solid phases

The soil profiles are composed of silty and clayey sediments exhibiting varying degrees of oxidation, as observed by measuring the pHf. In both profiles, the sediments were divided into three distinct zones based on their oxidation state: Reduced (pH>7), Transition (pH 4-7), and Oxidized (pH<4) (Fig. 5a). Beneath these zones, sandy sediments were present at the bottom of both profiles. These sands showed no signs of oxidation and had low S content (<0.01 %), suggesting no risk of acid generation.

Following the incubation experiment, the OZ samples showed no significant changes over time and maintained pH values below 4, confirming that these sediments were already fully oxidized. In contrast, over the TZ and RZ, it was possible to distinguish layers with significant decrease in pH during the incubation experiment. Both profiles displayed a significant sediment thickness (SW: 225 cm; SN: 432 cm), highlighting the potential to develop AAS-soils if the unoxidized layers are exposed to oxygen (Fig. 5b).

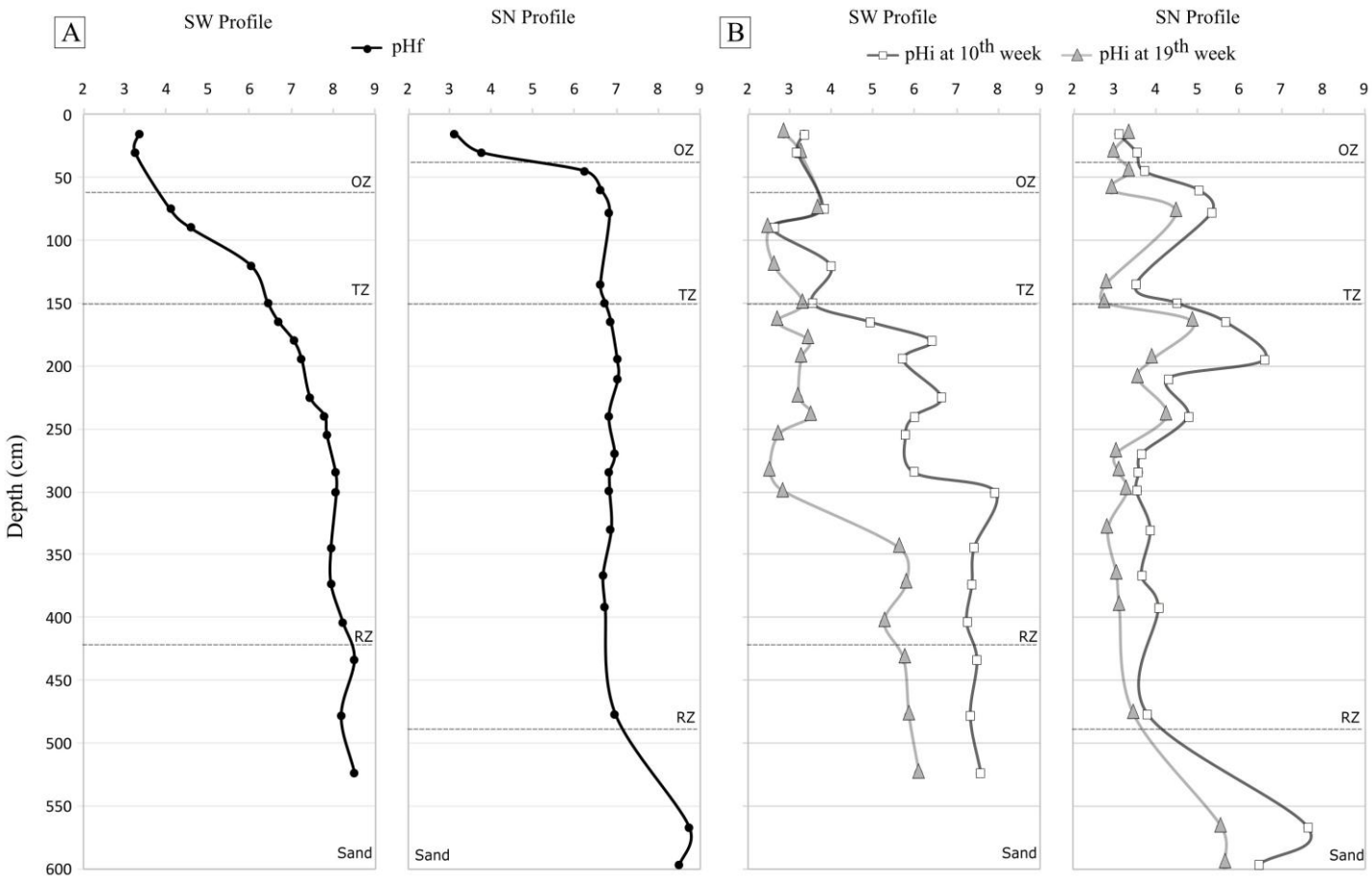

Fig. 5. (a) Field pH (pHf) measurements over the SW and SN soil profiles. (b) Variation of the incubation pH (pHi) at the 10th and 19th week over the soil profiles (Modified from Alvarellos et al., 2024).

3.1.1 Reduced Zone (RZ)

The RZ consists of unoxidized black-grey laminated sediments, characterized by alkaline pH values (>7) and high contents of TOC and S. The RZ represents the AS-soil parent material. In the RZ of the SW profile, it was possible to observe the highest concentrations of S (3.07 %), Mo (19.20 ppm), and TOC (3.35 %) (Fig. 6). Beneath the sediments enriched in S, Mo, and TOC, it was possible to identify the Ancylus Lake phase, which its sediments are characterized by low TOC, S, and Mo contents and the alternation of light and dark layers (E.g., monosulfides) Previous studies on the same study area, have described similar sediments from both the Littorina Sea and Ancylus Lake phases, confirming our assumptions (Fromm, 1965).

The incubation experiment showed that substantial quantities of sediment have the potential to generate acidity if they are exposed to oxygen. In addition, sequential extraction on the RZ samples demonstrates the potential of these sediments to release significant amounts of elements, such as Cd, Cu, Fe, Mn, Mo, and S, following oxidation processes, primarily associated with Fe sulfides and organic content.

The low pH in the OZ lead to element's mobilization such as Co, Fe, Mn, Ni, S, and Zn, resulting in their depletion and subsequent accumulation and/or precipitation in the TZ, where pH is higher, as observed in the SN profile (Fig.7). Similar distribution patterns throughout the soil profile were observed among Co, Ni, and Zn, as well as among Fe, Mn, and S, further supported by strong to very strong positive correlations values (Alvarellos et al., 2024).

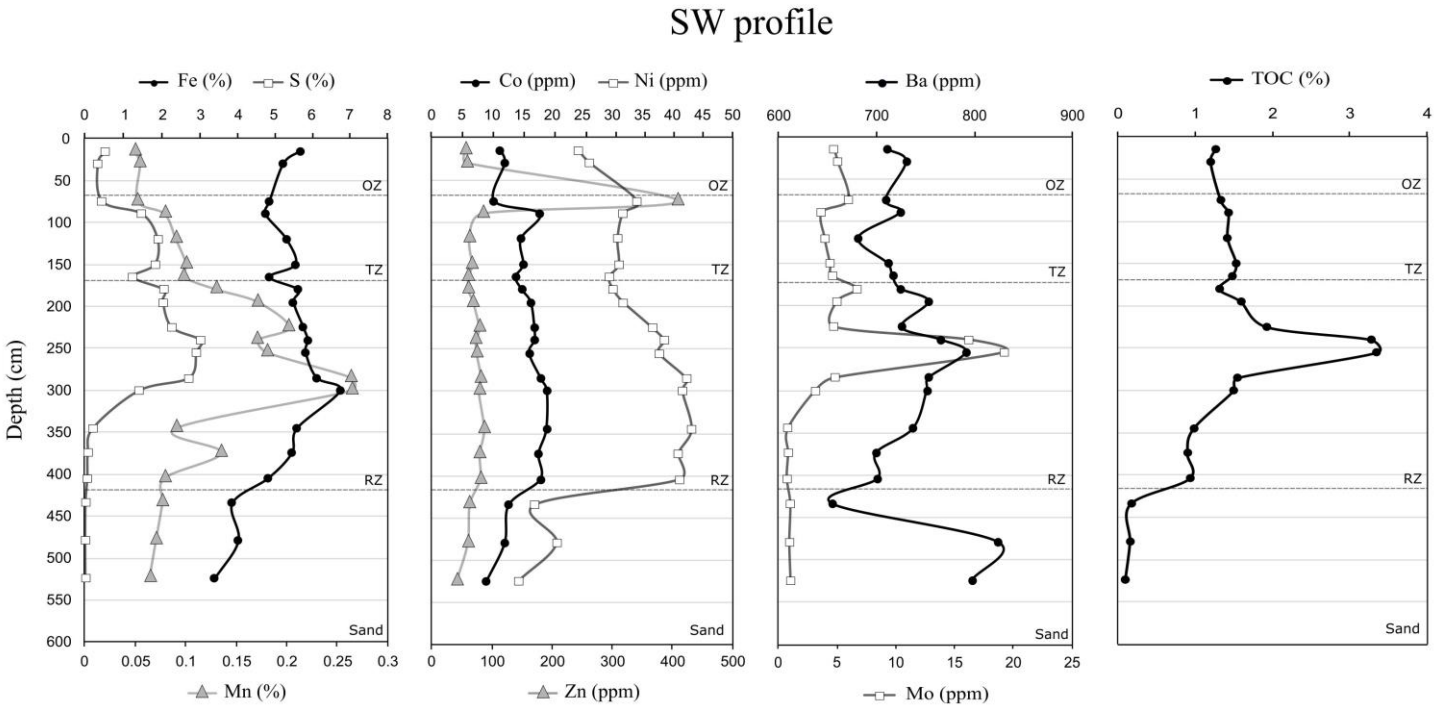

Fig. 6. Iron, S, Mn, Co, Ni, Zn, Ba, Mo, and TOC content in the SW profile (Modified from Alvarellos et al., 2024).

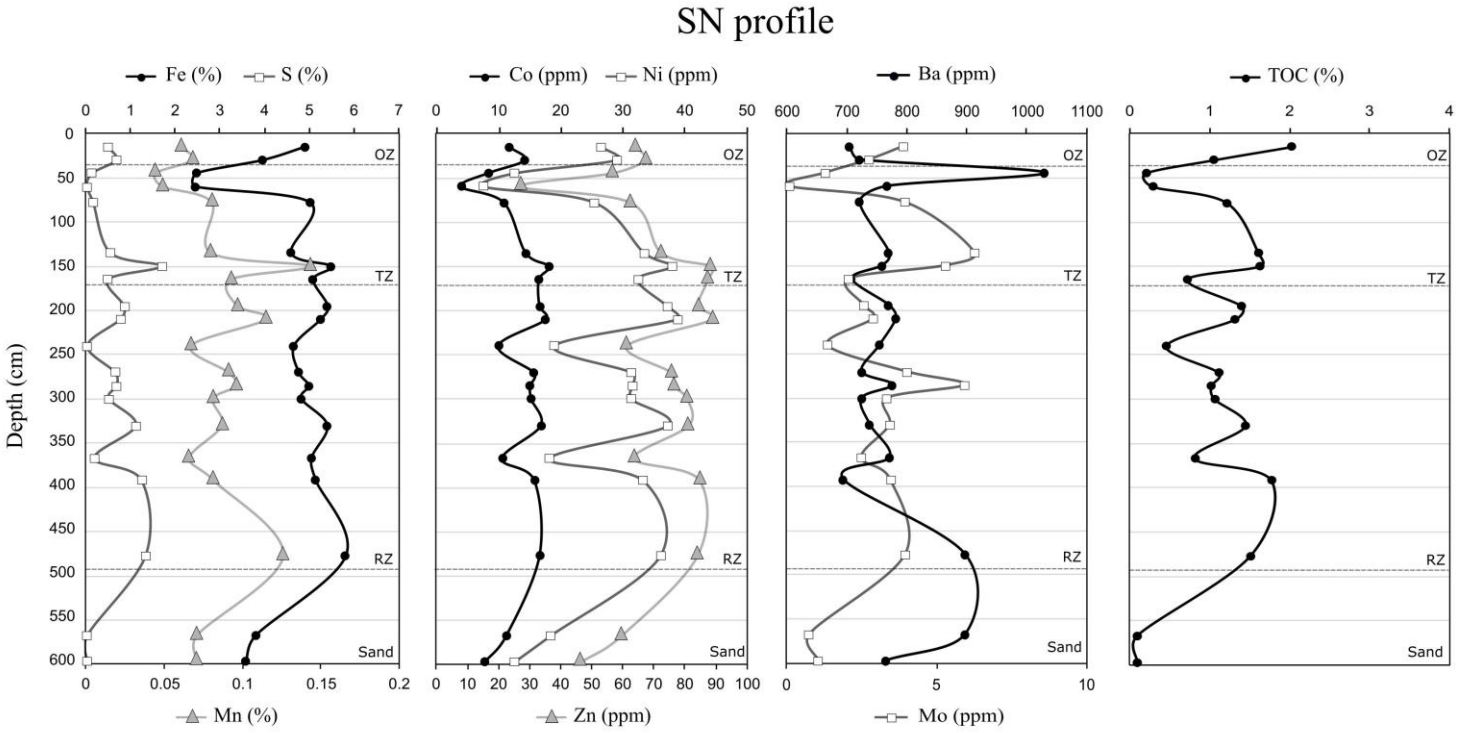

Fig. 7. Iron, S, Mn, Co, Ni, Zn, Ba, Mo, and TOC content in the SN profile (Modified from Alvarellos et al., 2024).

Primary Minerals: Framboidal pyrite with a Mn-rich rim

Mineralogical analysis using SEM-EDS imaging revealed that pyrite represents the most abundant primary Fe sulfide mineral in the RZ of both soil profiles. Pyrite is also present in the TZ, but to a lesser extent, and is absent in the OZ. In the RZ, pyrite appears predominantly as framboids, but it also occurs as nanoparticles, euhedral microcrystals, and secondary overgrowths on framboidal structures. Imaging by SEM-EDS and electron microprobe permitted the identification of different Fe sulfide mineral morphologies and textures, corresponding to different stages of framboidal pyrite formation as described in Alvarellos et al. (2024).

Framboidal pyrites are composed internally of hexagonal microcrystals (0.8 µm side), which can be either ordered or disordered arranged, with a rim between the microcrystals. In the RZ samples, it was possible to distinguish a Mn-rich rim (1 µm thick) surrounding the framboidal microcrystals (Fig. 8), a feature absent in the TZ as a consequence of oxidation. In addition, a bright outer layer with low S content, resembling metastable Fe sulfide (FeS), occurs, enclosing the entire framboid. Single framboids are predominant, although polyframboids with similar compositions were occasionally observed.

Framboid diameters are comparable between study sites but differ by depth. In the RZ, framboids are larger than those in the TZ. For instance, in the RZ-SN well, the average framboid diameter is 9.09 µm (SD: 1.60, n: 82), whereas in the TZ, is 6.85 µm (SD: 1.73, n: 10) (Fig. 9). The absence of oxidation in the RZ allows the framboids to remain intact, while partial oxidation in the TZ can contribute to pyrite dissolution and reduced framboid size.

Iron sulfide nanoparticles (<2 µm) containing Mn were observed with amorphous or heterogeneous morphologies. These nanoparticles occurred as isolated pseudo-crystals or as components of larger agglomerates. The agglomerates displayed a diffuse morphology, sub-rounded edges, complex structures, and a low degree of fracturing. Within this surface, hexagonal (0.4 µm side) and cubic (0.7 µm side) well-defined Fe sulfide microcrystals were identified. Secondary overgrowths of euhedral pyrite crystals were also observed, characterized by densely packed framboidal pyrites (without Mn) and cubic pyrite crystals (0.5 µm per side). These overgrowths exhibited a high degree of fracturing, the absence of Mn, and sharply defined, straight edges. In addition to mineralogical phases, microbiological remains were observed in the RZ, including diatom frustules and other round-shaped siliceous microfossils.

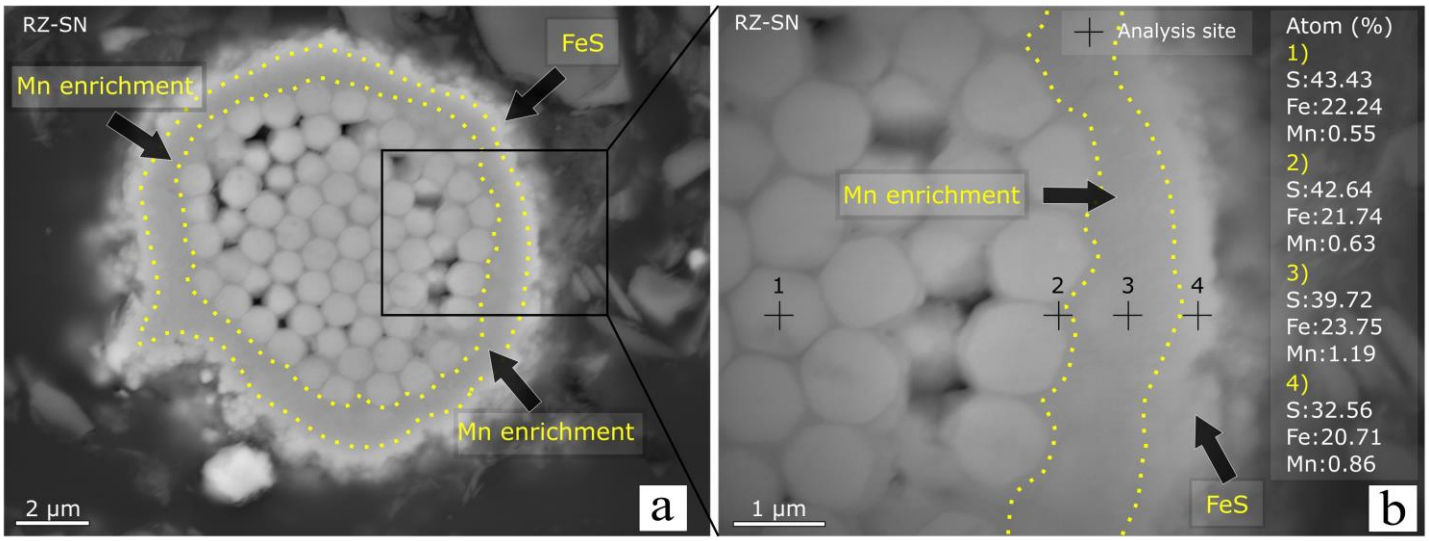

Fig. 8. (a) Backscattered electron image of a framboidal pyrite featuring an internal structure of hexagonal microcrystals and a Mn-rich outer rim from the RZ of the SN profile. (b) A high magnification image displaying the Mn-rich rim surrounding the framboid, along with compositional analysis (Modified from Alvarellos et al., 2024).

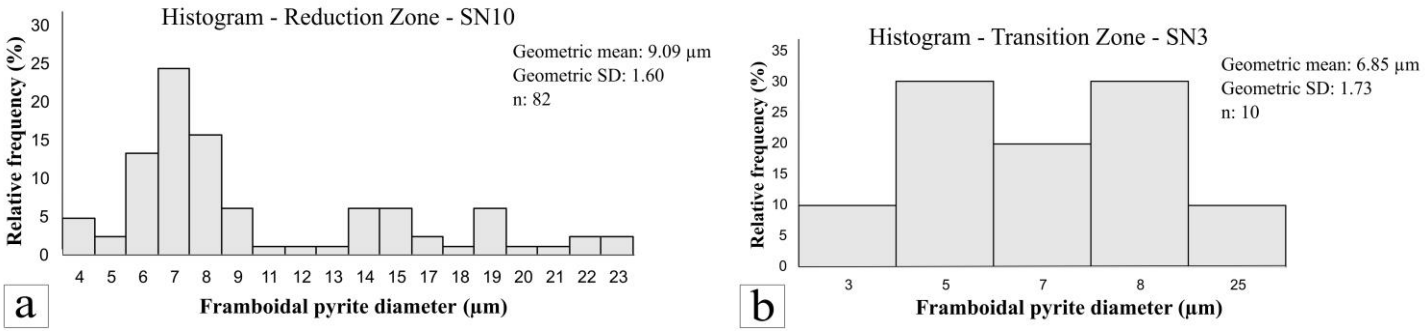

Fig. 9. (a) Histogram illustrating the diameter distribution of framboidal pyrite in the reduced zone (SN10 sample), accompanied by the geometric mean and standard deviation values. (b) Histogram illustrating the diameter distribution of framboidal pyrite in the transition zone (SN3 sample), accompanied by the geometric mean and standard deviation values.

Trace elements associated with pyrite

Compositional maps obtained through microprobe analysis, along with the results of the sequential extraction experiment, provide strong evidence that the oxidation of pyrite leads to the release of elements such as Co, Cu, Fe, Mn, Ni, and S into the environment (Fig. 10). The composition of framboidal pyrites varies slightly between profiles. The SW profile shows higher concentrations of As, Cd, Cr, Fe, Mo, and S, whereas the SN profile contains higher concentrations of Cu, Co, Mn, Ni, and Zn (Alvarellos et al., 2025a). Trace elements are generally distributed within the framboids, except for Mn, which concentrates at the edges of the framboid, creating a Mn-rich rim.

The sequential extraction experiment permitted the determination of the elements associated with the sulfide fraction (step 7) in the samples. In step 7, most elements exhibited leaching percentages below 15 %. The highest leaching percentages were observed for Ag, Mo, Sn, Th, Ti, and Zn, while Ca, Cd, and Si showed no detectable percentages. The release elements during step 7 are associated not only with pyrite but also with sphalerite and metastable Fe sulfides, which were previously identified (Alvarellos et al., 2024). Microprobe elemental mapping of framboidal pyrites from the RZ samples allowed for a detailed determination of pyrite composition. These framboidal pyrites contain measurable weight percentages (% wt) of Co, Cu, Mn, and Ni. Low percentages of As, Cd, Cr, Pb, and Zn were detected in some spot analyses, but most values were below detection limits.

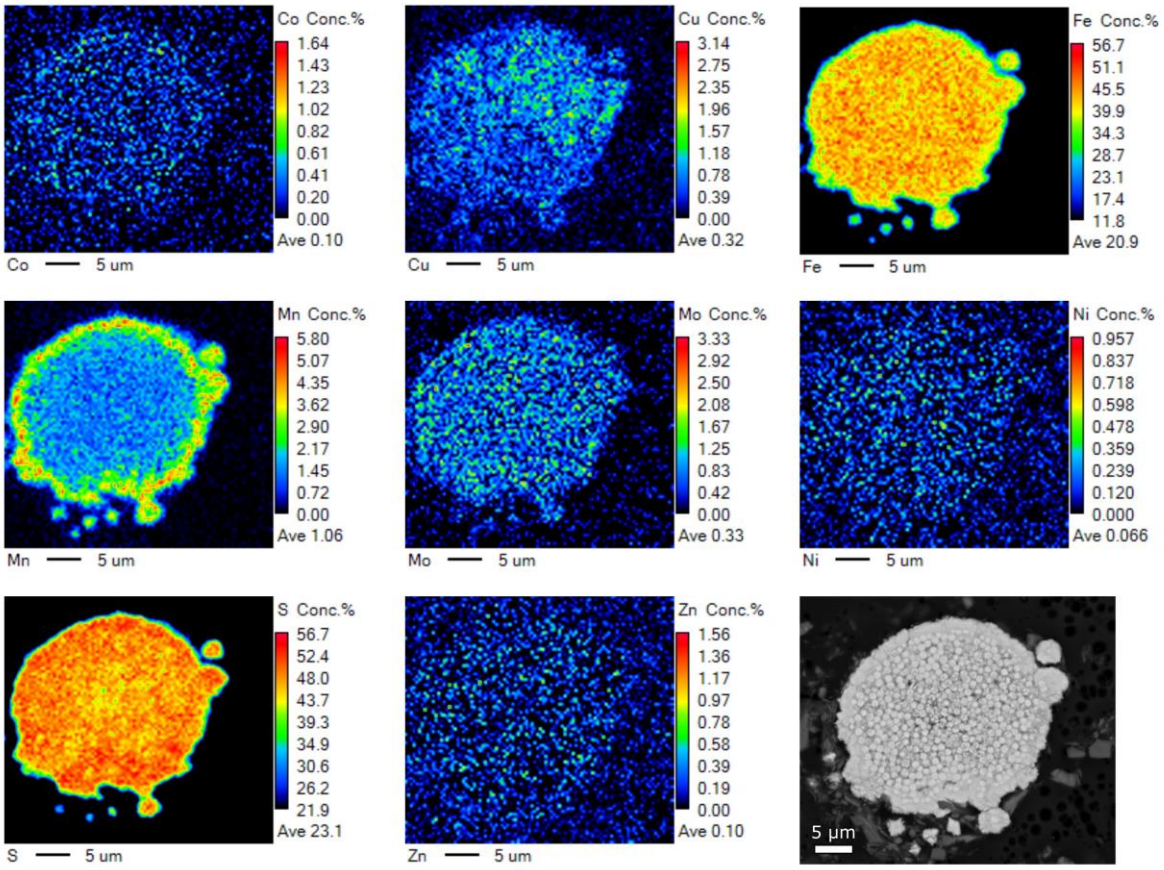

Fig. 10. Elemental compositional mapping obtained by microprobe, showing the distribution and quantification of Co, Cu, Fe, Mn, Mo, Ni, S, and Zn, within framboidal pyrite composition in the RZ-SW profile.

Organic matter

Organic matter is an important component of soil profiles, comprising both labile (E.g., humic and fulvic acids) and more stable organic compounds. In the RZ, organic matter is primarily associated with stable organic compounds, whereas the OZ is associated with the labile fraction.

Sequential extraction showed a significant finding: both the labile and stable organic fractions serve as a source of elements that can become bioavailable upon oxidation. In the stable organic fraction (step 6), S showed the highest leaching percentage, around 60 %, followed by Cu, Fe, Mn, and Mo, all exceeding 20 %, whereas the labile fraction (step 3) exhibited substantial release of Cu, Fe, Mn, Mo, and REE (Fig. 11). The elevated S content in the RZ suggests the presence of organic S as an important S species in the soil. These results highlight organic matter as an important source of Cu, Mo, and S during the oxidation of AS-soils.

Silicates

Samples from the OZ, TZ, and RZ of both soil profiles were analyzed using X-ray diffraction (XRD) to identify the silicate minerals. The dominant silicates were quartz, plagioclase (Mainly albite), K-feldspar (Microcline), aluminosilicate (Zeolites), micas (Biotite, muscovite), cordierite, and titanite. Quantitative analysis confirmed that quartz, albite, and microcline were the most abundant minerals, while the remaining minerals were present in quantities below 3 %. The distribution of silicate minerals was consistent across both profiles, with only minor variations in abundance and the appearance of a few alteration minerals, such as vermiculite, which was detected in the OZ and TZ of the SW profile.

Silicate minerals are highly resistant to weathering and represent the mineral phase that, for many elements, contains the highest contents, as confirmed by the sequential extraction. In the residual extraction step, most elements showed their highest leaching percentage, except S, which had already been dissolved in earlier steps. This suggests that most of these elements associated with silicates remain immobile unless exposed to extreme oxidative conditions.

The highest leaching percentages in the residual fraction were observed for Si and Al, consistent with their association with quartz, albite, and microcline. Iron and Mg also showed significant removal, with average leaching percentages exceeding 35 %, indicating their association with biotite, cordierite, and chlorite. Zirconium exhibited leaching percentages above 50 %, indicating zircon dissolution, a common accessory mineral in the sediments (Alvarellos et al., 2024). Titanium registered a leaching percentage exceeding 60 %, which is associated with titanite. The significant removal of Ba in this residual step further suggests its association with silicates, as previously noted (Alvarellos et al., 2024). Elements such as Co, Cu, and Mo showed leaching percentages below 15 %, indicating their presence as trace elements within the silicate structure (Fig. 11).

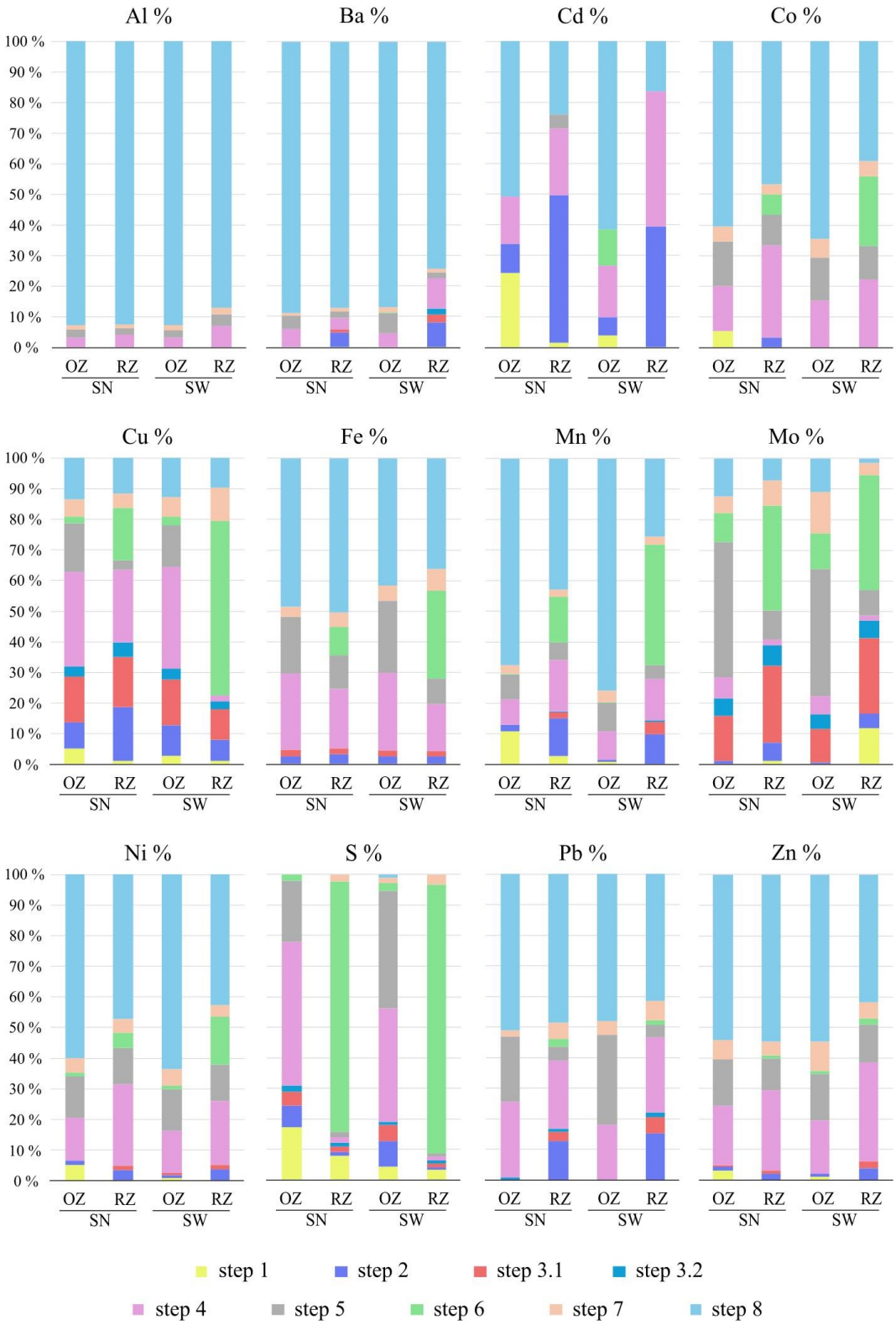

Fig. 11. Bar plot diagrams illustrating the extracted percentages of Al, Ba, Cd, Co, Cu, Fe, Mn, Mo, Ni, S, Pb, and Zn from oxidized (OZ) and unoxidized samples (RZ) of both AS-soil profiles (SN and SW) across the sequential extraction steps. Extraction steps: Step 1: H_2O-soluble; Step 2: Exchangeable, Step 3.1 and 3.2: Labile organics; Step 4: Easily reducible phase, Step 5: Moderately reducible phase, Step 6: Organics + sulfides, Step 7: Primary sulfides, Step 8: Silicates (Alvarellos et al., 2025a).

3.1.2 Transition Zone (TZ)

The TZ, or accumulation zone, in both soil profiles extends to a depth of approximately 150 cm. It is characterized by a distinct color change from orange-yellow in the overlying OZ to brown-gray, and higher pH values, ranging from 4 to 7, compared to the OZ. The increase in pH to near-neutral values within the TZ promotes the accumulation and precipitation of elements. This accumulation is evident in the SN profile, where elements such as Ba, Co, Fe, Mo, Ni, Pb, P, S, Ti, and Zn show marked enrichment within the TZ.

3.1.3 Oxidized Zone (OZ)

In both profiles, an OZ was identified, with a thickness of 30 cm in the SN profile and 60 cm in the SW profile. The permanently waterlogged condition in the SW profile suggests that its OZ was formed prior to the regulation of the Lule River in the seventies (Siergieiev et al., 2014) when unoxidized sediments were exposed to oxygen during periods of low groundwater levels. The OZ is characterized by acidic pH (<4) and yellow-reddish coloured sediments, indicative of secondary mineral precipitation such as Fe(oxy)hydroxides and/or Fe hydroxysulfate.

Although element mobilization during oxidation has already occurred in the OZ, results from sequential extraction experiments performed on both soil profiles indicate that the OZ still has the potential to release elements, even after initial oxidation (Fig. 11). Specifically, concentrations of Cd, Cu, Mn, Ni, S, and Zn in the OZ will become bioavailable under continued oxidation and element mobilization processes and washed-out during periods with high water level.

Secondary Minerals: Sulfates and Fe(oxy)hydroxides

Optical mineral analysis using a stereoscopic microscope on the OZ samples revealed the presence of yellow-orange precipitates, likely corresponding to Fe hydroxysulfate minerals such as jarosite or schwertmannite. Backscattered electron imaging further confirmed the presence of microcrystals (< 2 μm) of jarosite, identifying it as one of the dominant secondary Fe sulfate minerals in the OZ. Elemental profiles showed enrichment of Ba and Pb in the OZ, suggesting the precipitation of barite and anglesite. This was confirmed with SEM-EDS analysis, which identified euhedral barite and anglesite crystals, confirming their presence as secondary sulfate phases. The chemical compositions (In mass %) of jarosite and barite obtained with SEM-EDS were compared with reference data from the Web mineral database (webmineral.com) and previous mineralogical studies from the same area (Gunnarson et al., 2018).

This comparison illustrated using ternary plots of Fe, K, and S composition graph, demonstrated strong compositional agreement, confirming the minerals jarosite and barite, using ternary plots of Ba, S, and O (Fig. 12).

The reddish-orange coloration observed in the OZ sediments is attributed to Fe (oxy)hydroxides (FeOOH, $FeOH_3$) precipitates (E.g., ferrihydrite crystals) formed as a result of oxidation processes. Field observations and stereoscopic microscope analysis revealed minerals with distinct reddish and yellow colorations. Elemental mapping with SEM-EDS allowed for the differentiation of Fe and S concentrations, indicating the coexistence of Fe (oxy)hydroxides and Fe sulfates within the OZ.

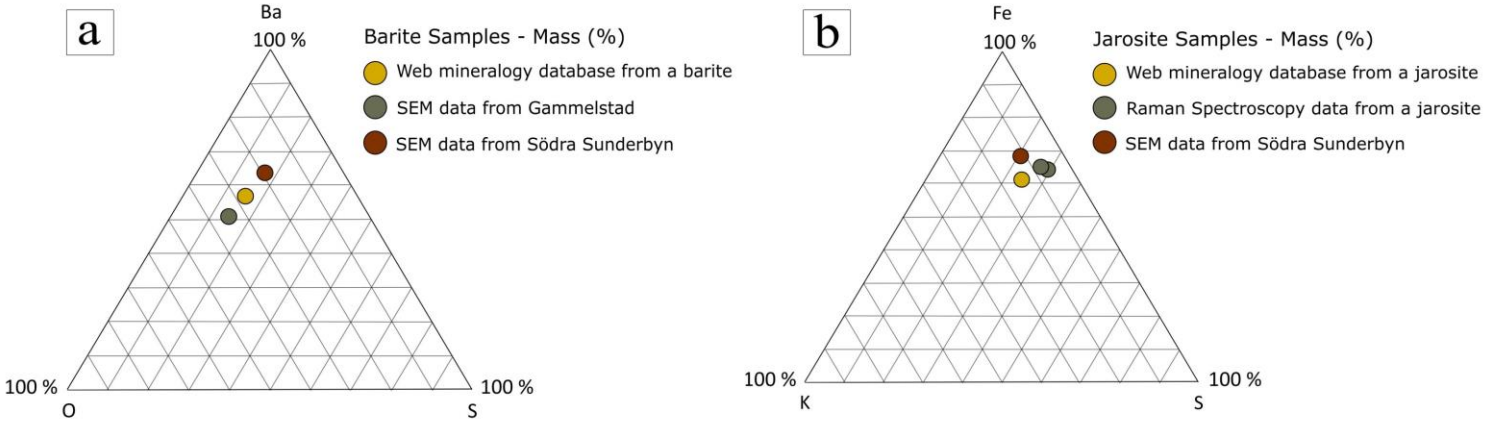

Fig. 12. (a) Triangular compositional diagram of Ba, O, and S illustrating the variations in barite sample compositions (Colville and Staudhammer, 1967). (b) Triangular compositional diagram of Fe, K, and S illustrating the variations in jarosite sample compositions (Becker and Gasharova, 2001).

During sequential extraction, the dissolution of the amorphous reducible soil fraction released significant quantities of elements, highlighting the role of Fe (oxy)hydroxides and sulfates as important mineral phases and source of trace elements under leaching. During the extraction, nearly all the elements showed measurable release with Ba, Co, Cu, Fe, Mo, Ni, S, Pb, and Zn (Fig. 11).

3.2. Geochemical variations in the groundwater

SN groundwater well

The SN well exhibited fluctuations in the water table, ranging from a maximum depth of 36 cm (October) to a minimum of 3 cm (July). The pH ranged from acidic to neutral, with the lowest values observed in May and October (Fig. 13). High concentrations of Al, Co, Fe, Mn, Ni, S, and Zn and dissolved SO_4^{2-} were registered during these acidic conditions (Fig. 14). During the study period, the SN well exhibited an increasing concentration trend in Na^+ and K^+ and anions such as HCO_3^-, resulting in a sodium bicarbonate facie of groundwater composition.

Dissolved oxygen presented low values in the SN well, remaining under low oxygen conditions over the study period. This is attributed to the high concentrations of DOC, which promotes oxygen consumption through microbial decomposition processes. The SN well showed higher concentrations of DOC, NH_4^+, and P, suggesting a potential anthropogenic influence, likely from agricultural activities due to the surrounding farming areas.

SW groundwater well

The SW well showed differences compared to the SN well in terms of element concentration patterns, parameters, and geochemical processes. The SW well maintained a relatively stable water table at ground level with minimal variation (Fig. 13). The pH remained consistently alkaline. The SW well is characterized by lower element concentration values compared to the SN well, due to the waterlogged condition, which prevents Fe sulfide oxidation. The elements do not show a clear concentration trend, except for Mo, which gradually decreased over the study period (Fig. 14). During the study period, the SW well showed a decrease in Cl^- concentration, maintaining high Na^+ - K^+ values, resulting in a sodium chloride facie.

The groundwater in the SW well gradually developed low oxygen conditions over the study period, evidenced by the LDO depletion, low DOC, and $NH4^+$ concentration. The gradual LDO depletion may be a result of bacteria that consume oxygen during organic matter decomposition. The DOC concentration was lower and exhibited less variation compared to the SN well. Both electrical conductivity and temperature vary slightly between the sites, sharing a similar trend over the study period (Fig. 13).

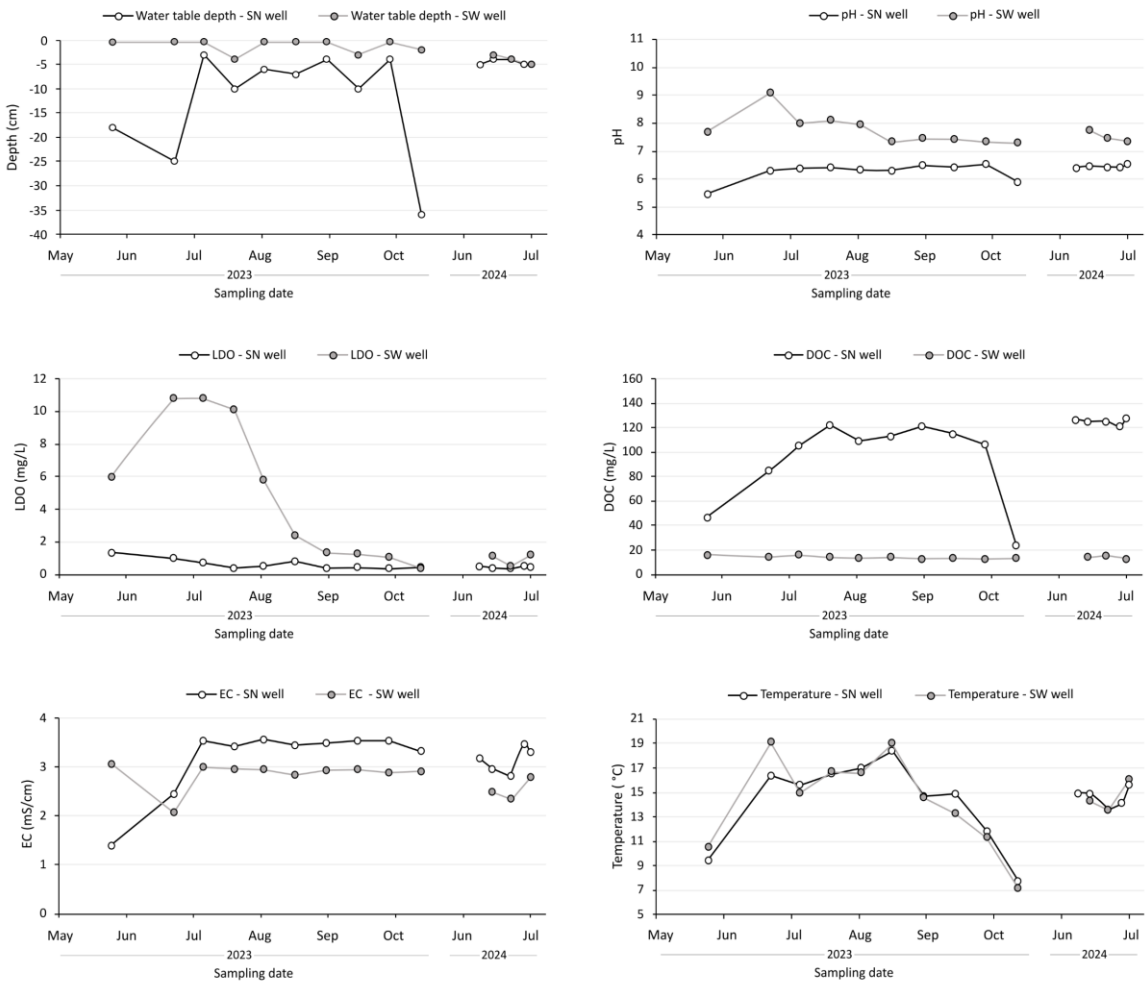

Fig. 13. Variation of groundwater table (cm), pH, LDO (mg/L), EC (mS/cm), DOC (mg/L), and Temperature (°C) in the SN and SW wells from May 2023 to June 2024. (Alvarellos et al., 2025b, in preparation).

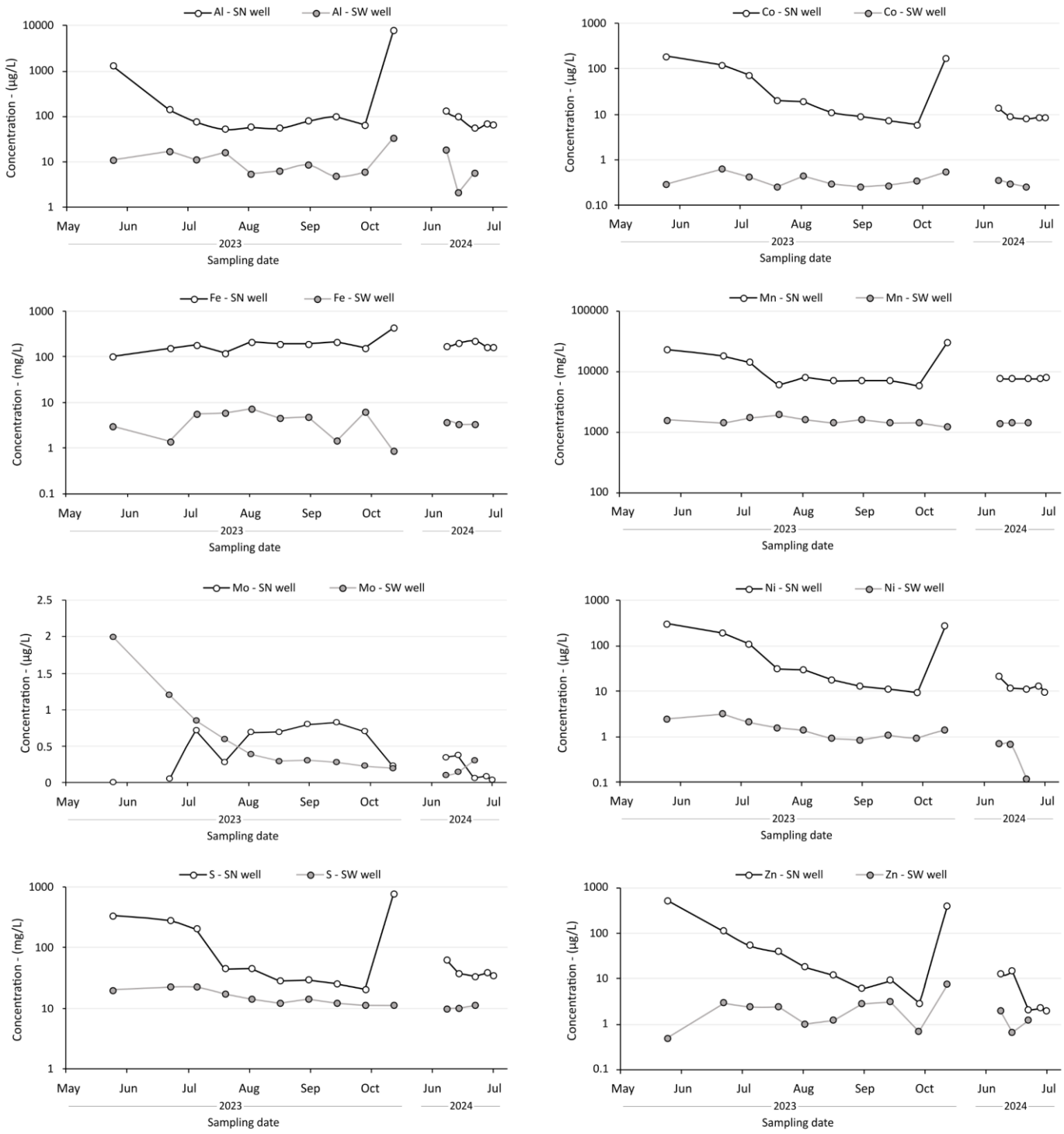

Fig. 14. Major, minor, and trace element concentrations of the SN and SW wells from May 2023 to June 2024. Note that the Y axis of Al, Co, Fe, Mn, Ni, S, and Zn has a logarithmic scale (Log10). (Modified from Alvarellos et al., 2025b, in preparation).

Fe/S ratio as redox indicator

The Fe/S ratio from groundwater concentrations can be used as a variability indicator in redox processes and in the geochemical dynamics of Fe and S; however, processes such as the Fe-bearing precipitation minerals or external sources of Fe and S can significantly influence this parameter. In the SW well, the Fe/S ratio ranged from 0.07 to 0.53, whereas in the SN well, it ranged from 0.29 to 8.24, suggesting the influence of different geochemical processes in each location (Fig. 15). To achieve a more comprehensive understanding of the geochemical processes, it would be important to complement the Fe/S ratio values with additional geochemical parameters, including pH, redox potential, S speciation, and mineral saturation indices.

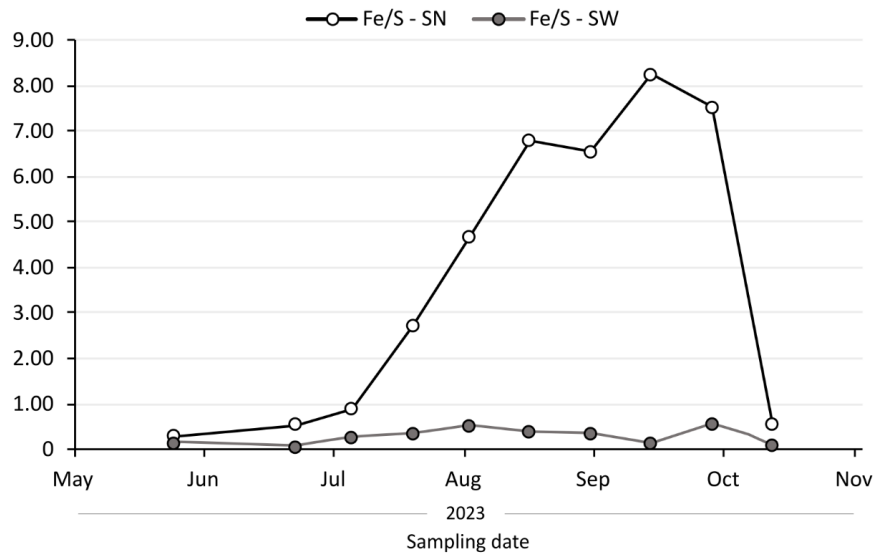

Fig. 15. Fe/S ratios over the study period from SN and SW groundwater wells (modified after Conrad et al., 2025, under review).

3.3 Isotopes

Fe and S isotopes in the solid phase

In the SW profile, the $\delta^{34}S$ is -7.7 ‰ at the OZ, decreases to -11.6 ‰ at the TZ, and reaches a minimum of -22.7 ‰ at 180 cm in the RZ, followed by a slight increase to -15.5 ‰ at 240 cm (Fig. 16). In contrast, the SN profile exhibits an alternating $\delta^{34}S$ pattern, with values of -7.9 ‰ at 30 cm, shifting to -0.5 ‰ at 60 cm, then returning to more negative values as -4.0 ‰ in the RZ, and once again approaching zero -0.7 ‰ at 240 cm (Fig. 16).

Despite minor fluctuations, $\delta^{56}Fe$ values remain relatively stable in both SW and SN profiles, ranging from 0.04 ‰ to 0.08 ‰ in SW, and from 0.05 ‰ to 0.16 ‰ in SN. (Fig. 16). Both profiles present similar $\delta^{56}Fe$ values, which align with the Fe isotope standard and fall within the range for crustal igneous rocks (+0.09 ± 0.08 ‰; Heimann et al., 2008; Teng et al., 2013; Du et al., 2017). These $\delta^{56}Fe$ values indicate that the Fe samples did not undergo significant isotopic fractionation.

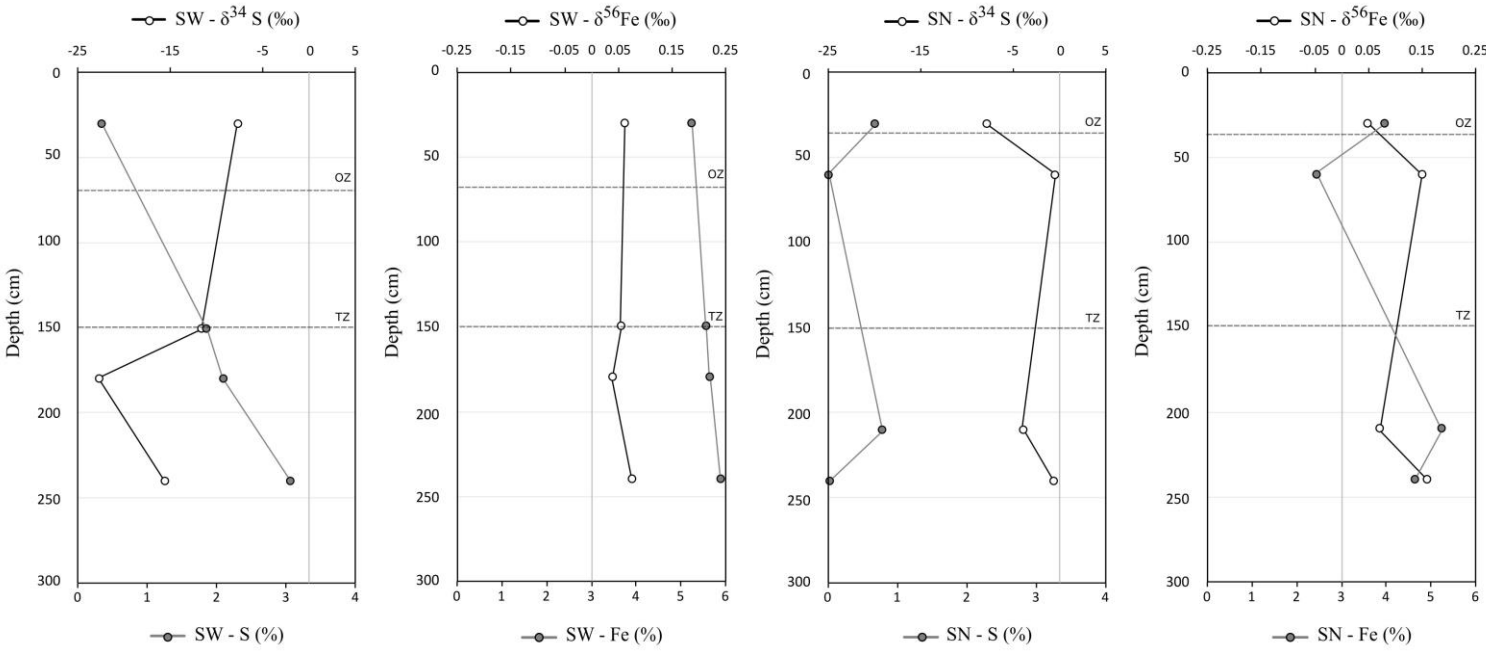

Fig. 16. Sulfur and Fe concentration and $\delta^{34}S$ and $\delta^{56}Fe$ isotope values in solid samples from the SN and SW profiles (modified from Conrad et al., 2025).

Fe and S isotopes in the sequential extraction experiment

Sequential extraction data reveal a progressive depletion in $\delta^{34}S$ across the analyzed mineralogical phases, indicating a transfer of lighter S isotopes from primary to secondary minerals due to sulfide oxidation (Table 2). A distinct pattern is observed in the SW-RZ, where positive $\delta^{34}S$ values in steps 2, 4, and 5 indicate limited sulfide oxidation and the retention of ^{34}S-enriched sulfate under stable, reducing conditions. This isotopic enrichment likely results from prior microbial sulfate reduction that preferentially removed ^{32}S, leaving behind a residual sulfate enriched in ^{34}S. These findings suggest the presence of a distinct S source in this zone.

The $\delta^{56}Fe$ values across the extraction steps show a much broader range (−1.96 ‰ to +0.97 ‰) than those in the bulk soil (Table 2). These heterogeneous values reflect the complex nature and variability of Fe in soils, which result from both lithogenic inputs and pedogenic processes that fractionate Fe isotopes (Fantle and DePaolo 2004, Thompson et al. 2007, Wu et al 2019).

Table 2. Isotope values of $\delta^{34}S$ and $\delta^{56}Fe$ from SN and SW solid samples at each step of the sequential extraction scheme. Isotopic ratios of Fe and S were not analyzed in Step 6 due to the instability and high reactivity of the hydrogen peroxide (H_2O_2) solutions. Sulfur isotopic analysis was not performed on the labile organic phase (Step 3) due to significant ^{31}P tailing on ^{32}S during extraction with sodium pyrophosphate ($Na_4P_2O_7$) (modified from Conrad et al., 2025).

	SN - SW Samples							
Extraction Steps	SN1 $\delta^{34}S$ (‰)	SN10 $\delta^{34}S$ (‰)	SW1 $\delta^{34}S$ (‰)	SW15 $\delta^{34}S$ (‰)	SN1 $\delta^{56}Fe$ (‰)	SN10 $\delta^{56}Fe$ (‰)	SW1 $\delta^{56}Fe$ (‰)	SW15 $\delta^{56}Fe$ (‰)
H_2O-soluble	-7.00	-7.16	-5.94	-3.65	-1.96	-1.83	-1.60	-1.13
Exchangable	-7.38	-6.00	-6.77	1.73	0.49	0.157	0.899	0.726
Labile organics (3.1)	-	-	-	-	0.356	0.213	0.902	0.775
Labile organics (3.2)	-	-	-	-	0.491	0.285	0.967	0.928
Labile organics (3.3)	-	-	-	-	-	-	-	-
Easily reducible phase	-11.4	-12.5	-8.08	4.79	0.27	0.924	0.523	0.532
Moderately reducible phase	-13.7	-13.4	-10.97	1.93	-0.207	0.030	0.130	0.005
Organics + Sulfides	-	-	-	-	-	-	-	-
Primary Sulfides	-3.96	-10.6	-7.40	-9.20	0.071	0.081	0.393	0.201
Silicates	-4.10	-8.28	-11.3	-2.68	0.175	0.193	0.079	0.168

Fe and S isotopes in groundwater

Over the study period, the SN well exhibited negative $\delta^{34}S$ isotopic values, with a gradual trend toward less negative values, indicating a progressive enrichment in ^{34}S, ranging from -8.36 ‰ to -5.39 ‰. In contrast, the SW well showed positive $\delta^{34}S$ values over the study period, increasing from 33.62 ‰ to 45.19 ‰, with an exception in July, during which a decline was observed (Fig. 17).

In both groundwater wells, $\delta^{56}Fe$ values were generally negative, with the exception of the SN well during the summer, which exhibited positive values. The SN well showed an enrichment ^{56}Fe trend, except for a sharp decrease (-1.06 ‰) in October. In the SW well, $\delta^{56}Fe$ values exhibit minor fluctuations over time without a clear trend, consistently remaining within a negative range from –0.07 ‰ to –0.56 ‰ (Fig. 17).

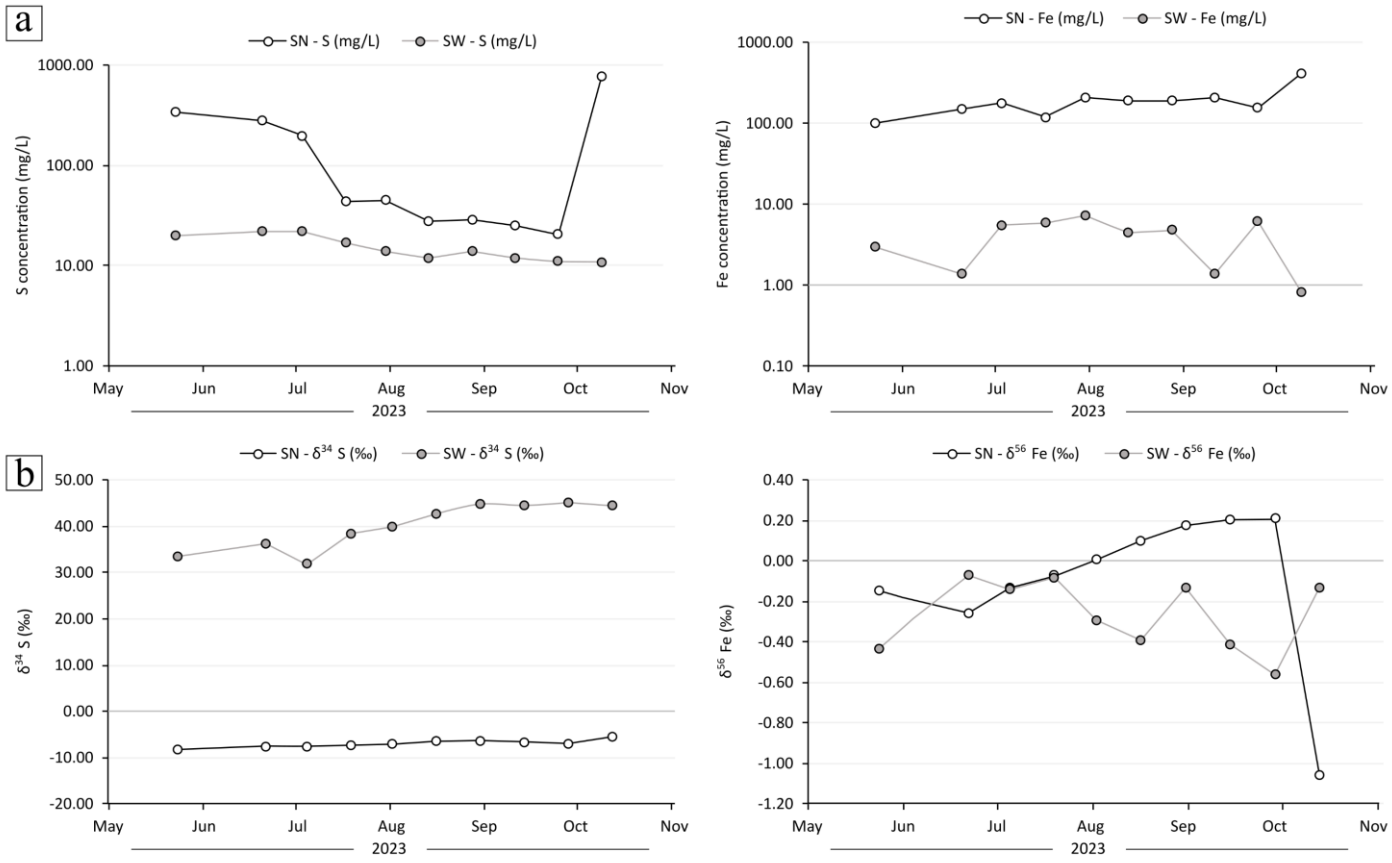

Fig. 17. (a) S and Fe concentration values in groundwater samples from the SN and SW profiles, measured from May to October. Note that the Y axis has logarithmic scale (Log10). (b) $\delta^{34}S$ and $\delta^{56}Fe$ isotope values in groundwater samples from the SN and SW profiles, measured from May to October. (modified from Conrad et al., 2025).

4. Discussion

4.1 Geochemical Behavior of Elements Under Dynamic Redox Conditions

This research provides a comprehensive understanding of the geochemical dynamics that govern the elements' behavior in AS-soils subjected to fluctuating redox environments. The results show that the mobilization of elements such as Al, Cd, Co, Cu, Fe, Mn, Ni, S, and Zn is strongly influenced by redox-sensitive processes, particularly those triggered by variations in groundwater levels. The TZ is notably influenced by water table fluctuations, which result in partially saturated and oxidized conditions. These redox dynamics lead to the oxidation of Fe sulfide minerals, as evidenced by lower pyrite content and secondary mineral precipitation.

In the SN well, high concentrations of Al, Co, Cu, Fe, Mn, Ni, S, and Zn were recorded during periods of low groundwater tables (Notably in May and October), in which acidic conditions prevailed as a result of sulfide oxidation. Under such conditions, the primary sulfide minerals oxidation, mainly framboidal pyrite, acts as a primary mechanism for the release of metals into the environment. In contrast, during periods of high groundwater levels (June to October), oxidation processes are significantly reduced or inhibited, leading to the stabilization or decline in the element concentrations. The persistently waterlogged conditions in the SW well further illustrate this mechanism, as low concentrations and minimal variations of elements were detected, reflecting limited oxidative mobilization. The low element concentrations are associated with processes such as immobilization, mineral precipitation, and/or adsorption onto mineral surfaces or organic matter. These observations are consistent with seasonal groundwater fluctuations described by Jarsjö et al. (2020), where water table changes enhance oxidation processes and mobilization of harmful metals from AS-soils into soil and water bodies.

The contrasting $\delta^{34}S$ isotopic signatures observed in groundwater from the two analyzed sites indicate the influence of distinct geochemical processes occurring in each well. In the SN well, negative $\delta^{34}S$ values indicate that sulfide oxidation predominates, with minimal microbial sulfate reduction (MSR). In contrast, positive $\delta^{34}S$ values in the SW well suggest ongoing MSR activity. The gradual trend toward positive $\delta^{56}Fe$ values in the SN well reflects the mobilization of Fe-rich phases under oxidizing conditions and associated isotopic fractionation. Under fluctuating redox conditions, the dissolution and transformation of Fe phases such as exchangeable Fe, labile organic-bound Fe, and amorphous Fe (oxy)hydroxides can release Fe enriched in ^{56}Fe into the groundwater, as the residual solid phases preferentially retain the lighter Fe isotope (^{54}Fe). The negative $\delta^{56}Fe$ values observed in the SN well during June and October are associated with low groundwater table conditions, where the oxidation of sulfide minerals releases Fe with lighter isotopic signatures into the groundwater. The negative $\delta^{56}Fe$ isotope values with minimal fluctuations in the SW well are consistent with reductive dissolution of Fe(III) phases and the release of light Fe isotopes associated with sulfide and organic matter under low oxygen conditions. Additionally, the Fe/S ratio permitted differentiate geochemical processes, suggesting oxidative processes at high ratios and reductive processes at low ratios.

During early oxidation, the most soluble soil fractions, particularly the water-soluble and exchangeable phases, play a significant role as important elements contributors, as evidenced by sequential extraction analyses. The high solubility of Ca, Cd, Cu, Mn, Mo, Pb, S, V, U, W, and REEs indicates their potential environmental availability in early oxidation stages. Moreover, pore water contributed with high contents of Al, Fe, Mn, S, V, and W, which were detected in TZ

and RZ samples, indicating their potential contribution under oxidation events (Alvarellos et al., 2025a).

Secondary minerals such as Fe-Al (oxy)hydroxide and sulfates have an important role as element contributors. During the sequential extraction, it was shown that oxidation of easily reducible phases releases high concentrations of Al, Cd, Co, Cu, Fe, Mo, Ni, Pb, S, and Zn, associated with (oxy)hydroxide phases. At the same time, the release of Ba, Fe, K, Pb, and S in particular from the OZ samples is attributed to the presence of secondary sulfate minerals such as jarosite, barite, and anglesite. The negative $\delta^{34}S$ values observed in step 4 also reflect the dominance of sulfide oxidation processes, wherein the release of dissolved sulfate leads to precipitation of jarosite. Similar results have shown that the $\delta^{34}S$ values of jarosite are comparable to those of the precursor sulfide (Field, 1966). The positive $\delta^{56}Fe$ values observed in step 4 of the OZ samples are associated with secondary (oxy)hydroxide and Fe hydroxysulfate minerals.

The highly resistant primary minerals, such as Fe oxides and silicates, are characterized by contributing high percentages of elements. However, due to their resistance to oxidation, the elements in their mineral structure are not easily available unless exposed to intense oxidative conditions. Iron oxides such as magnetite, hematite, and ilmenite were identified as contributors of Cu, Fe, Mn, Ni, Ti, and Zn as observed in the sequential extraction analyses (Alvarellos et al., 2025a). Signs of dissolution in crystalline Fe oxides were observed during the extraction step 4, which may explain the presence of Fe in the RZ samples (Alvarellos et al., 2025a). The observed −0.2‰ $\delta^{56}Fe$ value from the oxide extraction step further supports the contributions from ilmenite or magnetite derived from granitic rocks (E.g., Schuessler et al. 2009; Sossi et al. 2012; Telus et al. 2012; Foden et al. 2015; Du et al. 2017), as both minerals are commonly present in the profiles. Silicates contain the highest proportions of Al, Ca, Fe, K, Mg, Si, and Zr, as shown in the residual fraction of the sequential extraction process. In this residual step, the $\delta^{56}Fe$ values of +0.08 ‰ and +0.19 ‰ align closely with average crustal values and support the interpretation that this fraction primarily consists of refractory silicates and unreactive Fe-bearing minerals, such as biotite, commonly found in granitic rocks (E.g., Telus et al. 2012; Foden et al. 2015; Du et al. 2017).

4.2 Sulfur Speciation and Its Contribution to Acidity Generation

The speciation of S within the analyzed AS-soils is an important determinant of both the acid potential generation and the trace elements mobilization. This study confirms that framboidal pyrite is the predominant primary sulfide mineral. Anhedral and cubic pyrite crystals were also observed, but to a lesser extent. In addition, sulfide minerals such as sphalerite have been identified as euhedral crystals. Metastable Fe sulfides were observed as anhedral crystals in the RZ samples (Alvarellos et al., 2024). While elemental S^0 was not detected in the analyzed samples, it was identified in similar AS-soil profiles near the study area, where it appeared as euhedral crystals in partially oxidized samples from the TZ, as previously described (Gunnarsson, 2018). Elemental S^0 can precipitate as a final or partial oxidation product due to bacterial sulfide oxidation to sulfate (Taylor and Wirsen, 1997; Kelly, 1989; Werne et al., 2004). Sulfate phases are present as jarosite, barite, anglesite, and sulfate efflorescence salts identified in the OZ. The negative $\delta^{34}S$ values observed in steps 1 and 4 from the OZ samples are associated with secondary sulfate minerals, which reflect the isotopic signature of the parent primary sulfides (Mayer et al., 2010; Kilminster & Cartwright, 2011; Unland et al., 2012).

The presence of organic S compounds, as inferred from the substantial S extraction in the labile and organic phases, highlights the importance of organic matter in the S cycle of these soils. Organic S may exist in forms such as sulfide, polysulfide, or S^0 integrated within organic macromolecules. Although organic matter can contribute to acidification processes, incubation experiments revealed that pH decrease was more closely associated with layers containing high inorganic S content, even when TOC levels were not elevated (Alvarellos et al., 2024). These results corroborate the dominant role of pyrite oxidation as the principal source of acidity in the studied AS-soils.

Dissolved S species in groundwater, specifically SO_4^{2-} and S^{2-}, exhibited similar seasonal trends, with concentration increases when acidic conditions prevailed. The elevated SO_4^{2-} concentrations in the SN well, compared to the SW well, are directly associated with greater fluctuations in groundwater levels, promoting sulfide minerals oxidation.

Sequential extraction confirms that framboidal pyrite is highly reactive throughout the process and is particularly susceptible to rapid oxidation even with brief exposure to oxygen. Our findings indicate that pyrite shows signs of dissolution and a reduction in grain diameter prior to the sulfide extraction step. Metastable Fe sulfides and other S-containing species, such as elemental S^0 mentioned by Burton et al. (2006) and Gunnarsson (2018), also contribute to acidity when exposed to oxygen. This study demonstrates that the AS-soils in the study area contain various S species that contribute to acidity. Therefore, acidity potential estimation in risk assessments should account for the various S species as well as the contribution of organic matter present in sulfide-bearing sediments.

4.3 Characteristics of the AS-soil Parent Material

The parent material of the analyzed AS-soils is derived from unoxidized, laminated black–grey sediments deposited during the Littorina Sea stage of the Quaternary period, under euxinic to anoxic marine conditions. The parent material exhibits high S, Mo, TOC and abundant Fe sulfide minerals, indicative of sedimentary environments with limited oxygen availability and high rates of organic matter degradation and sulfate reduction. In particular, the RZ-SW profile (240–300 cm) displayed markedly elevated concentrations of Mo, S, and TOC, consistent with formation under sustained reducing conditions. Further evidence of these anoxic and sulfidic conditions was observed through pore water composition and sequential extraction analyses that revealed high percentages of Mo, V, and W in the RZ samples. The association of Mo, S, V, and W in anoxic, sulfidic marine environments, as observed in the RZ samples, has been well documented in several studies (Emerson and Huested, 1991; Calvert and Pedersen, 1993; Mohajerin et al., 2016).

Isotopic evidence further corroborates the depositional environment. The negative isotopic signature of $\delta^{34}S$ measured in the RZ samples suggests intensified reductive processes in RZ, associated with bacterial sulfate reduction to sulfide. The parent material was deposited under anoxic-euxinic conditions, influenced by processes such as MSR. Sulfate-reducing bacteria preferentially utilize the ^{32}S isotope in the production of H_2S, which is subsequently incorporated into sedimentary sulfides such as pyrite and leaves the residual S isotopically heavier (Kaplan and Rittenberg, 1964; Rickard, 2021; Raven et al., 2019). These findings align with those of Johnsson (2008) and Rickard (2021), who describe similar isotopic fractionation in sulfidic marine environments. The SW profile showed more negative values compared to the SN profile, suggesting more intense and sustained anoxic conditions in the SW profile, leading to greater

pyrite formation and S accumulation, as described in Alvarellos et al. (2024). The SN profile presents variability in Mo, S, and TOC content, alongside with alternation in $\delta^{34}S$ values reflecting fluctuation between anoxic and less anoxic conditions (Conrad et al., 2025, under review).

Negative $\delta^{56}Fe$ values from the sequential extraction experiment (step 1) indicate that the Fe in pore water originates from a different source than the other Fe phases. This Fe is associated with biogenic reduction of Fe(III) to Fe(II) (Wiederhold et al. 2007, Wu et al. 2019), a process that occurs during the formation of the AS-soil parent material (Alvarellos et al 2024). In the sulfide extraction step, the $\delta^{56}Fe$ values are attributed to Fe^{2+} in sulfides precipitated during the formation of the AS-soil parent material. The $\delta^{56}Fe$ values from this sulfide step coincide with those of the bulk samples. Additionally, $\delta^{56}Fe$ isotopic values from RZ-SW solid samples (−0.22 ± 0.04‰) support the interpretation of deposition under anoxic-euxinic conditions, consistent with findings by Severmann et al. (2008).

Isotopic fractionation is influenced by organic matter, which serves as an electron donor for sulfate-reducing bacteria, thereby facilitating MSR processes (Raven et al., 2019). This is evident in the RZ of both profiles since the SW well, which has high S % and high TOC, shows stronger isotopic fractionation. In contrast, the SN well, with lower S % and TOC, reflects reduced MSR due to limited organic matter. The negative $\delta^{34}S$ values in the OZ of both profiles suggest that secondary sulfate minerals incorporate isotopically light S derived from the oxidation of pyrite.

4.4 Role of Organic Matter

Organic matter has a significant influence on redox conditions and the mobility of elements within AS-soils. High levels of DOC recorded in the SN well correspond to persistently low concentrations of LDO, underscoring the role of organic carbon in promoting reducing conditions. In anoxic environments, microbial bacteria utilize electron acceptors such as NO_3^- and SO_4^{2-}, facilitating biogeochemical processes like MSR, which contribute to the formation of HCO_3^- and H_2S. This microbial reduction, as outlined by Berner (1985), is reflected in the increasing HCO_3^- concentrations in the SN groundwater composition and contributes to the formation of sodium bicarbonate facies.

The trace elements mobilization from the OZ to the TZ is associated with the decomposition of organic matter. An inverse relationship was observed between DOC and the concentration of several elements under acidic conditions in the SN well. Specifically, periods (May and October) of acidic pH and low DOC were associated with increased concentrations of Al, Ca, Co, Cu, Fe, Mn, Ni, S, and Zn. In contrast, higher DOC values corresponded with lower element concentrations in alkaline conditions (Alvarellos et al., 2025b, in preparation). These patterns indicate interactions between organic matter and specific elements, potentially involving adsorption mechanisms (Kaiser and Guggenberger, 2000) or the formation of organo-metal complexes (Kalbitz et al., 2005). In the solid phase, TOC, along with Co, Fe, Mn, Ni, S, and Zn, exhibited comparable content profiles and strong positive correlation values (Alvarellos et al., 2024). Sequential extraction results confirm that oxidation of organic-bound fractions (labile and stable) releases a significant amount of Cu, Co, Mn, Mo, Ni, S, and REE, highlighting organic matter as a key reservoir of potentially mobile elements.

Soil profiles and the incubation experiment facilitated the identification of sediment layers with acidifying potential. Both AS-soil profiles revealed substantial sediment thicknesses in the TZ and RZ that could pose an acid-risk environmental concern. Despite the important role of organic matter, its contribution to acidity generation is relatively minor when compared to pyrite. Incubation experiments revealed that layers with the highest acidification potential did not always correspond to those with the highest TOC, reinforcing the conclusion that pyrite oxidation is the dominant driver of acidification. Nevertheless, organic matter remains an important factor in shaping redox conditions and controlling the mobility of elements within AS-soil environments.

4.5 Mitigation Strategies for AS-soils

Monitoring of the groundwater table is important, as its fluctuations lead to alternation of dry and wet periods that generate oxidation processes with subsequent negative environmental impacts. An effective strategy to mitigate the AS-soils oxidation is to maintain the sulfide-bearing sediments under waterlogged conditions. Maintaining elevated groundwater tables through controlled hydrological management can significantly limit oxygen ingress and suppress acid generation (Österholm et al., 2015). This research demonstrates that waterlogged profiles maintain a stable alkaline pH and exhibit low concentrations of dissolved elements over time.

The minimization of disturbance to sulfide-bearing soils represents an important measure to prevent adverse environmental impacts. The incubation experiment demonstrates the significant environmental risks associated with the unoxidized layers of AS-soils. Both the RZ and TZ are characterized by elevated concentrations of harmful elements and highly reactive sulfide minerals. These zones have the potential to generate negative environmental impacts immediately upon exposure to oxygen. This study demonstrates that even short-term exposure is sufficient to initiate sulfide oxidation and the subsequent release of harmful elements.

A potential mitigation strategy involves the controlled incorporation of alkalizing agents or organic matter into the soil to increase pH and reduce metal solubility. This approach aims to change geochemical conditions that promote the elements' precipitation and adsorption, thereby leading to their immobilization. For instance, under neutral and alkaline conditions, elements such as Al, Cu, Fe, and Zn may precipitate into hydroxides or organic matter complexes (Åström and Corin, 2000; Nystrand et al., 2016). The sequential extraction experiment in this research shows that elements such as Al, Co, Fe, Mn, Ni, and Zn are present in easily exchangeable phases, making their chemical stabilization important. While mitigation experiments were not conducted in the present study, it is recommended that future research incorporates such experiments to achieve a more comprehensive understanding of the soil's mineralogical composition.

4.6 Future studies

This study is characterized by its detailed research of high-thickness sulfide sediment profiles from both geochemical and mineralogical perspectives. Therefore, the application of detailed geochemical and mineralogical analyses, such as those presented in this study, in future research on AS-soils would allow for a more accurate assessment of their potential to cause negative environmental impacts. Additionally, it would contribute to a deeper understanding of their mineralogical composition and associated geochemical processes.

As this study demonstrates that acidity generation is influenced not only by pyrite but also by organic matter and other S species, it would be valuable to conduct a more in-depth investigation into the role of S species such as polysulfides and S^0, whose presence and transformations can significantly impact acidity dynamics.

The impact of climate change on groundwater table fluctuations highlights the importance of developing predictive models that can integrate climatic, hydrological, and geochemical variables. Such models would facilitate the effective assessment and implementation of mitigation strategies, including controlled waterlogging and the application of alkaline amendments or organic matter.

5. Conclusions

This study presents a comprehensive case study on Swedish AS-soils, emphasizing the value of an integrated and multidisciplinary approach to their analysis. By combining soil geochemistry, mineralogical characterization, sequential chemical extractions, groundwater monitoring, and Fe–S isotope analysis, this research contributes meaningfully to global efforts to improve the assessment of the negative environmental impacts associated with AS-soils.

The analyzed AS-soils are particularly thick and exhibit a high potential for oxidation, leading to acid generation and the release of elements such as Cu, Co, Fe, Mn, Ni, S, and Zn. A temporal comparison between oxidized and waterlogged AS-soil profiles demonstrates that maintaining these soils under water-saturated conditions is an effective mitigation strategy. Water table management significantly minimizes environmental risks by limiting oxidation processes and thereby reducing both acid formation and element mobilization.

Detailed mineralogical analysis of framboidal pyrite reveals critical insights into its compositional heterogeneity and significant role as a primary source of acidity and element contributor. The high oxidative reactivity of framboidal pyrite indicates the high susceptibility of sulfidic sediments to oxidation, even under limited oxygen exposure.

This research highlights the importance of analyzing the organic fraction and including it in risk assessments. Although organic matter can contribute to acidity generation, this study found it to be a significant source of elements such as Cu, Mo, and S, indicating its influence on the bioavailability and mobility of these elements in the environment.

Climate variations induce water table fluctuations, leading to alternating wet and dry periods that promote sulfide oxidation processes, making seasonal groundwater changes a primary driver of both acidity and element release. Even brief episodes of oxygen exposure can cause substantial acidification, emphasizing the critical importance of hydrological stability in AS-soil management. This study confirms the major influence of groundwater dynamics in regulating oxidation processes and elemental mobility in AS-soils, reinforcing global concerns about the susceptibility of these environments to climate change.

References

Alvarellos, F., Conrad, S., Öhlander, B., Alakangas, L., 2024. Geochemical and mineralogical characterization of acid sulfate soils in Luleå, northern Sweden. Journal of Geochemical Exploration. Volume 265, 107541. https://doi.org/10.1016/j.gexplo.2024.107541.

Alvarellos, F., Rodiouchkina, K., Conrad, S., Öhlander, B., Alakangas, L., 2025a. Sources of Element Release from Acid Sulfate Soils to the Environment: Elemental and Mineralogical Evidence from Northern Sweden. https://doi.org/10.1016/j.apgeochem.2025.106571.

Alvarellos, F., Conrad, S., Öhlander, B., Alakangas, L., 2025b. Seasonal variability in groundwater hydrogeochemistry in acid sulfate soils, northern Sweden. (Manuscript in preparation).

Andriesse, W., van Mensvoort, M.E.F., 2006. Acid sulfate soils: distribution and extent. In: Encyclopedia of Soil Science, 2nd edition. Taylor & Francis group, New York, pp. 14–19.

Åström, M. E., Roos, P M. 2022. Geochemistry of multiple sclerosis in Finland. Science of the Total Environment, 841: 156672. https://doi.org/10.1016/j.scitotenv.2022.156672.

Åström, M., 1998. Partitioning of transition metals in oxidised and reduced zones of sulphide-bearing fine-grained sediments. Appl. Geochem. 13, 607-617. https://doi.org/10.1016/S0883-2927(97)00093-0.

Åström, M., 2001a. Abundance and fractionation patterns of rare earth elements in streams affected by acid sulphate soils. Chemical Geology 175 (3–4), 249–258. https://doi.org/10.1016/S0009-2541(00)00294-1.

Åström, M., 2001b. Effect of widespread severely acidic soils on spatial features and abundance of trace elements in streams. Journal of Geochemical Exploration 73: 181–191. https://doi.org/10.1016/S0375-6742(01)00196-0

Åström. M., Bjorklund. A., 1995. Impact of acid sulfate soils on stream water geochemistry in western Finland. J. Geochem. Explor. 55 (1–3). 163–170. https://doi.org/10.1016/0375-6742(95)00018-6.

Åström. M., Corin. N., 2000. Abundance, sources and speciation of trace elements in humus-rich streams affected by acid sulphate soils. Aquat. Geochem. 6 (3). 367–383. https://doi.org/10.1023/A:1009658231768.

Becher, M., Sohlenius, G., Öhrling, C., 2019. Sur sulfatjord – egenskaper och utbredning. (in swedish) SGU-rapport 2019:13.

Becker, U., Gasharova, B., 2001. Physics and Chemistry of Minerals , 28 p.545-556, AFM observations and simulations of jarosite growth at the molecular scale:, probing the basis for the incorporation of foreign ions into jarosite, as a storage mineral

Berner, R.A. 1985. Sulphate reduction, organic matter decomposition and pyrite formation. Phil. Trans. R. Soc. Lond. A 315, 25-38. https://doi.org/10.1098/rsta.1985.0027.

Boman, A., Fröjdö, S., Backlund, K., Åström, M.E., 2010. Impact of isostatic land uplift and artificial drainage on oxidation of brackish-water sediments rich in metastable iron sulfide. Geochem. Cosmochim. Acta 74, 1268–1281. https://doi.org/10.1016/j. gca.2009.11.026.

Bottrell S., Tellam J., Bartlett R. and Hughes A., 2008. Isotopic composition of sulfate as a tracer of natural and anthropogenic influences on groundwater geochemistry in an urban sandstone aquifer, Birmingham, UK. Appl. Geochem. 23, 2382–2394. DOI:10.1016/j.apgeochem.2008.03.012

Burton, E. D., Bush, R. T., Sullivan, L. A., 2006. Elemental sulfur in drain sediments associated with acid sulfate soils. Appl. Geochem. 21, 1240–1247. https://doi.org/10.1016/j.apgeochem.2006.02.020.

Burton, E.D., Karimian, N., Johnston, S.G., Schoepfer, V.A., Choppala, G., Lamb, D., 2021. Arsenic-imposed effects on schwertmannite and jarosite formation in acid mine drainage and coupled impacts on arsenic mobility. ACS Earth Sp. Chem. 5, 1418–1435. https://doi.org/10.1021/acsearthspacechem.1c00047.

Calvert, S.E., Pedersen, T.F., 1993. Geochemistry of recent oxic and anoxic sediments: implications for the geological record. Mar. Geol. 113, 67-88. https://doi.org/10.1016/0025-3227(93)90150-T.

Conrad, S., Rodiouchkina, K., Alvarellos, F., Öhlander, B., Alakangas, L., 2025. Isotopic insights into iron and sulfur cycling in acid sulfate soils: Implications of seasonal redox fluctuations. (Under review)

Colville., A. A., Staudhammer, K., 1967. American Mineralogist , 52 p.1877-1880, A refinement of the structure of barite, from Cow Green mine

Deng, H., Åström, M., Björklund, A., 1998. Geochemical and mineralogical properties of sulfide-bearing fine-grained sediments in Finland. Environ. Geol. 36, 37–44. https:// doi.org/10.1007/s002540050318.

Dent. D.L., Pons. L.J., 1995. A world perspective on acid sulfate soils. Geoderma 67. 263-276 https://doi.org/10.1016/0016-7061(95)00013 E.

Drugge, L., Jonsson, K., Wörman, A., Öhlander, B., 2003. Effect of hydropower regulation on the transport of metals and nutrients in Lule River. Uppsala. https://doi.org/10.1007/s10498-013-9215-6.

Du, D.H., Wang, X.L., Yang, T., Chen, X., Li, J.Y., Li, W.Q., 2017. Origin of heavy Fe isotope compositions in high-silica igneous rocks: a rhyolite perspective. Geochim Cosmochim Acta 218:58–72. https://doi.org/10.1016/j.gca.2017.09.014.

Emerson, S.R., Huested, S.S., 1991. Ocean anoxia and the concentrations of molybdenum and vanadium in seawater. Mar. Chem., 34, 177-196. https://doi.org/10.1016/0304-4203(91)90002-E.

Fältmarsch, R., Åström, M., Vuori K.-M., 2008. Environmental risks of metals mobilised from acid sulphate soils in Finland: a literature review. Boreal Environ. Res. 13, 444-456.

Fanning, D.S., Rabenhorst, M.C., Fitzpatrick, R.W., 2017. Historical developments in the understanding of acid sulfate soils. Geoderma 308, 191–206. https://doi.org/10.1016/j. geoderma.2017.07.006.

Fantle, M. S., DePaolo, D. J., 2004. Iron isotopic fractionation during continental weathering. Earth Planet. Sci. Lett. 228, 547–562. https://doi.org/10.1016/j.epsl.2004.10.013.

Fekiacova, Z., Montagne, D., Duvivier, A., Guilhou, A., Deschamps, P., Cornu, S., 2021. Evolution of Retisol impacted by artificial drainage: What can we learn from stable Fe isotope ratios? Geoderma 384, 114771. https://doi.org/10.1016/j.geoderma.2020.114771.

Field, C.W., 1966, Isotopic methods for discriminating between sulfates of hypogene and supergene origin: Econ. Geol., v. 61, p. 1428-1435.

Filter J, Jekel M, Ruhl A.S., 2017. Impacts of accumulated particulate organic matter on oxygen consumption and organic micro-pollutant elimination in bank fltration and soil aquifer treatment. Water 9(5):349. https://doi.org/10.3390/w9050349

Foden, J., Sossi, P. A., Wawryk, C. M., 2015. Fe isotopes and the contrasting petrogenesis of A-, I-and S-type granite. Lithos 212, 32–44. https://doi.org/10.1016/j.lithos.2014.10.015.

Fromm, E., 1965. Beskrivning till jordartskartan över Norrbottens län nedanför lappmarksgränsen. (in swedish) Sveriges geologiska undersökning Ca 39, 236 s.

Geological Survey of Sweden. https://www.sgu.se/om-sgu/nyheter/2023/maj/miljofarlig-sur-sulfatjord-ar-mer-utbredd-an-vad-man-tidigare-trott/ . Last accessed: 2023-10-06.

Gjorup, D.F., Schaefer C.E.G.R., Simas, F.N.B., Francelino, M.R., Michel, R.F.M., Bockheim, J.G., 2020. Sulfurization, acid-sulfate soils and active layer monitoring at the semiarid Seymour Island, Antarctica. Geoderma Reg 22: e00305. https://doi.org/10.1016/j.geodrs.2020.e00305.

Gröger, J., Proske, U., Hanebuth, T.J.J., Hamer, K., 2011. Cycling of trace metals and rare earth elements (REE) in acid sulfate soils in the Plain of Reeds, Vietnam. Chem. Geol. 288, 162–177. https://doi.org/10.1016/j.chemgeo.2011.07.018.

Gunnarsson, N., 2018. Mineralogical speciation of sulfur in acid sulfate soils from Luleå, Sweden. Natural Resources Engineering, Master's. Department of Civil, Environmental and Natural Resources Engineering. Luleå University of Technology.

Heimann, A., Beard, B. L., Johnson, C. M., 2008. The role of volatile exsolution and sub-solidus fluid/rock interactions in producing high 56Fe/54Fe ratios in siliceous igneous rocks. Geochim. Cosmochim. Acta 72, 4379–4396. https://doi.org/10.1016/j.gca.2008.06.009.

Hudd. R. and Kjellman. J.: Bad matching between hatching and acidification: a pitfall for the burbot. Lota lota. off the river Kyrönjoki. Baltic Sea. Fish. Res., 55. 153–160. https://doi.org/10.1016/S0165-7836(01)00303-4. 2002.

Jarsjö. J., Andersson-Sköld, Y., Fröberg, M., Pietroń, J., Borgström, R., Lov, Å., Kleja, D.B., 2020. Projecting impacts of climate change on metal mobilization at contaminated sites–Controls by the groundwater level. Sci. Total Environ. 712, 135560 https://doi. org/10.1016/j.scitotenv.2019.135560.

Johansson, M.M., Kahma, K.K., Boman, H., Launiainen, J., 2004. Scenarios for sea level on the Finnish coast. Boreal Environ. Res. 9, 153-166. ISSN: 1239-6095.

Johnson, C.M., Beard, B.L., Roden, E.E., 2008. The Iron Isotope Fingerprints of Redox and Biogeochemical Cycling in Modern and Ancient Earth. Annual Review of Earth and Planetary Sciences 36, 457-493.

Johnston, S.G., Slavich, P.G., Hirst, P., 2003. Alteration of groundwater and sediment geochemistry in a sulfidic backswamp due to *Melaleuca quinquenervia* encroachment.Aust. J. Soil Res. 41, 1343–1367. https://doi.org/10.1071/SR03027.

Kaiser, K., & Guggenberger, G. 2000. The role of DOM sorption to mineral surfaces in the preservation of organic matter in soils. Organic Geochemistry, 31(7–8),711–725. https://doi.org/10.1016/S0146-6380(00)00046-2.

Kalbitz, K., Schwesig, D., Rethemeyer, J., & Matzner, E. 2005. Stabilization of dissolved organic matter by sorption to the mineral soil. Soil Biology and Biochemistry, 37(7), 1319–1331. https://doi.org/10.1016/j.soilbio.2004.11.028.

Kaniuth, K., Vetter, S., 2004. GPS Estimates of postglacial uplift in Fennoscandia. Zeitchrift für Geodäsie. Geoinform. Landmanage. 129, 168-175.

Kaplan, I. R., Rittenberg, S. C., 1964. Microbiological fractionation of sulphur isotopes. Microbiology 34, 195–212. https://doi.org/10.1099/00221287-34-2-195.

Kelly, D.P., 1989, Oxidation of sulphur compounds, *in* Cole, J.A., and Ferguson, S., eds., The nitrogen and sulphur cycles: Society for General Microbiology Symposium 42, Cambridge University Press, p. 65-98.

Kemeny, P. C., Li, G. K., Douglas,M., Berelson, W., Chadwick, A. J.,Dalleska, N. F., et al., 2023. Arctic permafrost thawing enhances sulfide oxidation. Global Biogeochemical Cycles, 37, e2022GB007644. https://doi.org/10.1029/2022GB007644

Kilminster, K., Cartwright, I., 2011. A sulfur-stable-isotope-based screening tool for assessing impact of acid sulfate soils on waterways. Mar. Freshw. Res. 62, 152–161.

Lindström, C., 2017. Acid Sulfate Soils and Metal Accumulation in Sediments in the Rosån Catchment, Northern Sweden. Degree Project at the Department of Earth Sciences. Uppsala University. ISSN 1650-6553.

Lotfi-Kalahroodi, E., Pierson-Wickmann, A., Guénet, H., Rouxel, O., Ponzevera, E., Bouhnik-Le Coz, M., Vantelon, D., Dia, A., Davranche, M., 2019. Iron isotope fractionation in iron-organic matter associations: Experimental evidence using filtration and ultrafiltration. Geochim. Cosmochim. Acta 250, 98–116. https://doi.org/10.1016/j.gca.2019.01.036.

Love, L.G., 1957. Microorganisms and the presence of syngenetic pyrite. Q. J. Geol. Soc. Lond. 113, 429-440.

Mayer, B., Shanley, J.B., Bailer, S.W., Mitchell, M.J., 2010. Identifying sources of stream water sulfate after a summer drought in the Sleepers River watershed (Vermont, USA) using hydrological, chemical and isotopic techniques. Appl. Geochem. 25, 747–754.

Michel, R.F.M., Schaefer, C.E.G.R., Poelking, E.L., Simas, F.N.B., Fernandes Filho, E.I., Bockheim, J., 2012. Active layer temperature in two Cryosols fromKing George Island, Maritime Antarctica. Geomorphology. 155–156, 12–19. https://doi.org/10.1016/j.geomorph.2011.12.013.

Mohajerin, T.J., Helz, G.R., Johannesson, K.H., 2016. Tungsten-molybdenum fractionation in estuarine environments. Geochim. Cosmochim. Acta 177, 105–119. https://doi.org/10.1016/j.gca.2015.12.030.

Nyman, A., Johnson, A., Yu, C., Sohlenius, G., Becher, M., Dopson, M., Åström, M., 2023. A nationwide acid sulfate soil study — a rapid and cost-efficient approach for characterizing large-scale features. Sci. Total Environ. 869, 161845 https://doi.org/ 10.1016/j.scitotenv.2023.161845.

Nystrand, M. I., Österholm, P., Yu, C., and Åström, M. 2016. Distribution and speciation of metals, phosphorus, sulfate and organic material in brackish estuary water affected by acid sulfate soils, Appl. Geochem., 66, 264–274, https://doi.org/10.1016/j.apgeochem.2016.01.003.

Nystrand, M., Österholm , P., 2013. Metal species in a Boreal river system affected by acid sulfate soils. Applied Geochemistry 31. 133-141. https://doi.org/10.1016/j.apgeochem.2012.12.015.

Öborn, I., 1991. Some effects of chemical weathering in three cultivated acid sulfate soils in Sweden. In: Wright, R.J., Baligar, V.C., Murrmann, R.P. (Eds.), Plant - Soil Interactions at Low PH. Springer Netherlands, Dordrecht, pp. 55–63. https://doi. org/10.1007/978-94-011-3438-5_6.

Öborn, I., 1994. Morphology, Chemistry, Mineralogy and Fertility of Some Acid Sulfate Soils in Sweden. Ph D Dissertation. Department of Soil Sciences. Reports and Dissertations 18. Swedish University of Agricultural Sciences, Uppsala.

Öborn. I., 1989. Properties and classification of some acid sulfate soils in Sweden. Geoderma 45. 197– 219. https://doi.org/10.1016/0016-7061(89)90007-4.

Ódri Á., Becker M., Broadhurst J., Harrison S. T.L., Edraki M., 2020. Stable isotope imprints during pyrite leaching: implications for acid rock drainage characterization. Minerals 10, 982. https://doi.org/10.3390/min10110982.

Öhlander, B., Nordblad, F., Lax, K., Ecke, F., Ingri, J., 2014. Plant geochemical mapping of stream plants to trace acid sulphate soils: a comparison between water geochemistry and metal content in macrophytes. Geochemistry-Exploration Environment Analysis vol. 14, 1: 85-94. https://doi.org/10.1144/geochem2013-206

Österholm, P., Virtanen, S., Rosendahl, R., Uusi-Kämppä, J., Ylivainio, K., Yli-Halla, M., Mäensivu, M., Turtola, E., 2015. Groundwater management of acid sulfate soils using controlled drainage, by-pass flow prevention, and subsurface irrigation on a boreal farmland, Acta Agriculturae Scandinavica, Section B — Soil & Plant Science, 65:sup1, 110-120. DOI: 10.1080/09064710.2014.997787.

Österholm, P., Åström, M., 2004. Quantification of current and future leaching of sulfur and metals from Boreal acid sulfate soils, western Finland. Aus. J. Soil Res. 42(5-6), 547-551. https://doi.org/10.1071/sr03088.

Raab, B., Vedin, H., 1995. Klimat, sjöar och vattendrag, Sveriges Nationalatlas. (in swedish) SMHI, SNA Förlag

Raven, M. R., Fike, D. A., Bradley, A. S., Gomes, M. L., Owens, J. D., & Webb, S. A. (2019). Paired organic matter and pyrite δ 34 S records reveal mechanisms of carbon, sulfur, and iron cycle disruption during Ocean Anoxic Event 2 Earth and Planetary Science Letters, 512, 27-38. https://doi.org/10.1016/j.epsl.2019.01.048

Rickard, D., 2021. Framboids. Oxford University Press, First ed. Doi:10.1093/oso/9780190080112.003.0011

Schoepfer, V.A., Burton, E.D., 2021. Schwertmannite: a review of its occurrence, formation, structure, stability and interactions with oxyanions. Earth Sci. Rev. 221, 103811 https://doi.org/10.1016/j.earscirev.2021.103811.

Schuessler, J. A., Schoenberg, R., Sigmarsson, O., 2009. Iron and lithium isotope systematics of the Hekla volcano, Iceland—evidence for Fe isotope fractionation during magma differentiation. Chem. Geol. 258, 78–91. https://doi.org/10.1016/j.chemgeo.2008.06.021.

Seal R. R., Alpers C. N., Rye R. O., 2000. Stable isotope systematics of sulfate minerals. Reviews in Mineralogy and Geochemistry 40, 541–602. doi: https://doi.org/10.2138/rmg.2000.40.12

Shahabi-Ghahfarokhi, S., Åström, M., Yu, C., Lindquisit, T., Djerf, H., Kalbitz, K., Ketzer, M., 2022. Extensive dispersion of metals from hemiboreal acid sulfate soil into adjacent drain and wetland. Appl. Geochem. 136. https://doi.org/10.1016/j.apgeochem.2021.105170

Siergieiev, D., Widerlund, A., Lundberg, A., Almqvist, L., Collomp, M., Ingri, J., Öhlander, B., 2014. Impact of Hydropower Regulation on River Water Composition in Northern Sweden. Aquat Geochem 20, 59–80. https://doi.org/10.1007/s10498-013-9215-6.

Sohlenius, G., 1996. The history of the Baltic proper since the Late Weichselian deglaciation as recorded in sediments. PhD thesis. Quaternaria Ser A No 3. Stockholm University, 1-34.

Sohlenius, G., Öborn, I., 2004. Geochemistry and partitioning of trace metals in acid sulphate soils in Sweden and Finland before and after sulphide oxidation. Geoderma. 122, 167-175. https://doi.org/10.1016/j.geoderma.2004.01.006

Sohlenius. G., Aroka. N., Wåhlén. H., Uhlbäck. J., Persson. L., 2015. Sulfidjordar och sura sulfatjordar i Västerbotten och Norrbotten. (in swedish) Sveriges Geologiska Undersökni ng. SGU Rapport. 26.

Sossi, P.A., Foden, J.D., Halverson, G.P., 2012. Redox-controlled iron isotope fractionation during magmatic differentiation: an example from the Red Hill intrusion, S. Tasmania. Contrib Mineral Petrol 164:757–772. https://doi.org/10.1007/s00410-012-0769-x.

Swedish Meteorological and Hydrological Institute (SMHI). https://www.smhi.se/data/hitta-data-for-en-plats/ladda-ner-vaderobservationer (accessed 3 March 2025).

Taylor, C.D., Wirsen, C.O., 1997, Microbiology and ecology of filamentous sulfur formation: Science, v.277, p. 1483-1485, doi: 10.1126/SCIENCE.277.5331.1483.

Telus, M., Dauphas, N., Moynier, F., Tissot, F.L., Teng, F.Z., Nabelek, P.I., Craddock, P.R., Groat, L.A., 2012. Iron, zinc, magnesium and uranium isotopic fractionation during continental crust differentiation: the tale from migmatites, granitoids, and pegmatites. Geochim Cosmochim Acta 97:247–265. https://doi.org/10.1016/j.gca.2012.08.024.

Teng, F., Dauphas, N., Huang, S., Marty, B., 2013. Iron isotopic systematics of oceanic basalts. Geochim. Cosmochim. Acta 107, 12–26. https://doi.org/10.1016/j.gca.2012.12.027.

Thompson, H., Keenan, F. P., Dufton, P. L., Trundle, C., Ryans, R., Crowther, P. A., 2007. Iron abundances from optical Fe iii absorption lines in B-type stellar spectra. Monthly Notices of the Royal Astronomical Society 383, 729–740. https://doi.org/10.1111/j.1365-2966.2007.12597.x.

Unland, N.P., Taylor, H.L., Bolton, B.R., Cartwright, I., 2012. Assessing the hydrogeochemical impact and distribution of acid sulfate soils, Heart Morass, West Gippsland, Victoria. Appl. Geochem. 27, 2001–2009.

van Breemen, N, 1980. Acid sulphate soils. Problem soils: their reclamation and management. Land Reclamation and Water Management. ILRI Pub. 27, Wageningen (1980), pp. 53-57

Virtasalo, J. J., Österholm, P., Kotilainen, A. T., Åström, M. E., 2020. Enrichment of trace metals from acid sulfate soils in sediments of the Kvarken Archipelago, eastern Gulf of Bothnia, Baltic Sea, Biogeosciences, 17, 6097–6113, https://doi.org/10.5194/bg-17-6097-2020.

Vithana, C.L., Sullivan, L.A., Burton, E.D., Bush, R.T., 2015. Stability of schwertmannite and jarosite in an acidic landscape: prolonged field incubation. Geoderma 239, 47–57. https://doi.org/10.1016/j.geoderma.2014.09.022

Web mineral database. https://webmineral.com/. Last accessed: 2025-12-02.

Werne, J.P., Hollander, D.J., Lyons, T.W., Sinninghe Damsté, J.S., 2004. Organic sulfur biogeochemistry: Recent advances and future research directions, in Amend, J.P., Edwards, K.J., and Lyons, T.W., eds., Sulfur biogeochemistry -Past and present: Boulder, Colorado, Geological Society of American Special Paper 379, p. 135-150.

White, I., Melville, M.D., Sammut, J., Wilson, B.P., Bowman, G.M., 1996. Downstream impacts from acid sulphate soils. In: Eyles, A., Hunter, H. and Rayment, G. (eds), Downstream Effects. pp. 165–172. Queensland Dept. Natural Resour., Brisbane.

Wiederhold, J. G., Teutsch, N., Kraemer, S. M., Halliday, A. N., Kretzschmar, R., 2007. Iron isotope fractionation in oxic soils by mineral weathering and podzolization. Geochimica et Cosmochimica Acta 71, 5821–5833. https://doi.org/10.1016/j.gca.2007.07.023.

Wilkin, R.T., Barnes, H.L., 1997. Formation processes of framboidal pyrite. Geochim. Cosmochim. Acta 61(2), 323-339. https://doi.org/10.1016/S0016-7037(96)00320-1.

Wu, B., Amelung, W., Xing, Y., Bol, R., Berns A. E., 2019. Iron cycling and isotope fractionation in terrestrial ecosystems. Earth-Sci. Rev. 190, 323–352. https://doi.org/10.1016/j.earscirev.2018.12.012.

Yuan, C., Fitzpatrick, R., Mosley, L.M., Marschner, P., 2015. Sulfate reduction in sulfuric material after re-flooding: effectiveness of organic carbon addition and pH increase depends on soil properties. J. Hazard. Mater. 298, 138–145. https://doi.org/10.1016/j.jhazmat.2015.05.013.

Department of Civil, Environmental, and Natural Resources Engineering
Division of Applied Geochemistry

ISSN 1402-1544
ISBN 978-91-8048-771-9 (print)
ISBN 978-91-8048-772-6 (pdf)

Luleå University of Technology 2025

LULEÅ
UNIVERSITY
OF TECHNOLOGY